

# **THESIS**

**HASNA SAADI**  
**Mechanical engineering**

**Gödöllő**  
**2023**



**Hungarian University of Agriculture and Life Science**  
**Szent István Campus**  
**Mechanical engineering Course**

**SOLAR ENERGY UTILISATION WITH THE HEAT PUMPS**

**Primary Supervisor:** Emőd Péter KORZENSZKY, PhD.  
habil. associate professor  
Péter HERMANUCZ, PhD.

**Independent Consultant:**

**Author:** **Hasna Saadi**  
XTNU6K

**Institute/Department: Institute of Technology**

**Gödöllő**  
**2023**

**INSTITUTE OF TECHNOLOGY MECHANICAL ENGINEERING (MSC)**  
**Technical development specialization**

**THESIS**  
worksheet for

*Hasna SAADI (XTNU6K)*

---

(MSc) student

**Entitled:**

**Solar energy utilization with the heat pumps**

---

**Task description:**

Build a solar-assisted heat pump system, and investigate the change of the outlet temperature of the solar collector in the function of the inlet temperature in the same solar irradiation ranges over three days of experiments, as well as the impact of the ambient temperature in the same solar irradiation ranges and same inlet temperature of the solar collector over the same three days of experiments, Simulating the solar collector model by using MATLAB Simulink and comparing the predicted outlet temperature by MATLAB and the measured one.

**Department: Mechanical Engineering**

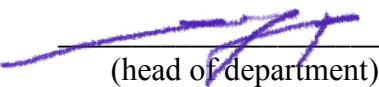
**Consultant:**

**Supervisor:** Dr. Emőd Péter KORZENSZKY Associate Professor, MATE, Institute of Technology

**Submission deadline:** 09 May 2023.

Gödöllő, 20 January 2023.

**Approved**

  
(head of department)

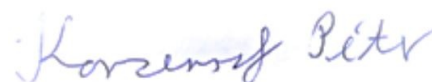
  
(host course leader)

**Received**

  
(student)

As an independent consultant of the author of this thesis I hereby declare that the student took part in the planned consultations.

Gödöllő, 08 May 2023.



(Consultant)

## Table of contents

|         |  |    |
|---------|--|----|
| 1       | Introduction.....  | 6  |
| 2       | Literature review .....  | 7  |
| 2.1     | Introduction to literature review .....                                | 7  |
| 2.2     | Direct expansion solar-air source heat pump system .....               | 7  |
| 2.2.1.1 | Indirect expansion solar-assisted heat pump .....                      | 10 |
| 2.2.2   | Indirect expansion single-source solar-assisted heat pump system.....  | 11 |
| 2.2.3   | Indirect expansion double-source solar-assisted heat pump system ..... | 19 |
| 2.2.3.1 | solar assisted air-source heat pump system .....                       | 19 |
| 2.2.3.2 | solar assisted ground-source heat pump system .....                    | 22 |
| 2.3     | Modelization.....  | 24 |
| 2.3.1   | Mathematical modeling of a solar-assisted heat pump system .....       | 25 |
| 2.3.1.1 | Solar Thermal Collectors .....   | 25 |
| 2.3.1.2 | Heat Pump .....  | 26 |
| 2.4     | Conclusion.....  | 28 |
| 3       | Materials and methods .....  | 29 |
| 3.1     | Description of the materials.....                                      | 29 |
| 3.1.1   | Solar collector .....  | 29 |
| 3.1.2   | Heat Pump .....  | 30 |
| 3.1.2.1 | Compressor .....   | 30 |
| 3.1.2.2 | Condenser .....  | 31 |
| 3.1.2.3 | Expansion valve.....   | 31 |
| 3.1.2.4 | Heat exchanger-Evaporator .....  | 31 |
| 3.1.2.5 | Storage tank .....   | 31 |
| 3.1.2.6 | Control system.....  | 31 |
| 3.1.3   | Data collection material .....   | 31 |
| 3.1.3.1 | ALMEMO system .....  | 32 |
| 3.1.3.2 | The solar irradiation instruments .....                                | 32 |
| 3.1.3.3 | The temperature sensors instruments .....                              | 32 |
| 3.1.3.4 | Amper clamp meter .....  | 33 |
| 3.2     | Description of the methods.....  | 33 |
| 3.2.1   | The schema of the executed solar-assisted heat pump system.....        | 33 |
| 3.2.2   | The use of the ALMEMO system .....                                     | 34 |
| 3.3     | Simulation.....  | 34 |
| 3.3.1   | MATLAB software.....   | 34 |

|         |   |    |
|---------|---|----|
| 3.3.1.1 | The chosen mathematical model .....   | 34 |
| 4       | Results and Discussion .....  | 36 |
| 4.1     | The measured External Conditions.....   | 36 |
| 4.2     | The measured outlet temperature of the solar collector.....                         | 38 |
| 4.2.1   | The outlet temperature under (780-910W/m <sup>2</sup> ) of solar irradiation .....  | 38 |
| 4.2.2   | The outlet temperature under (780-910W/m <sup>2</sup> ) of solar irradiation .....  | 40 |
| 4.2.3   | The outlet temperature under (910-1040W/m <sup>2</sup> ) of solar irradiation ..... | 41 |
| 4.2.4   | The outlet temperature under (1040-1170W/m <sup>2</sup> ) of solar irradiation..... | 43 |
| 4.3     | The extracted heat and coefficient of performance (COP).....                        | 45 |
| 4.4     | MATLAB Simulink Results .....   | 48 |
| 4.5     | Comparisons with previous works .....   | 49 |
| 5       | Conclusion .....  | 51 |
| 6       | Summary .....   | 52 |
|         | References .....  | 56 |
|         | Appendix .....  | 60 |

# 1 Introduction

To meet the demand for a high-quality life, i.e., a comfortable living and working environment, and convenient and efficient travel modes, a significant quantity of energy, i.e., coal, petroleum, and electricity, has been consumed, resulting in an assault of carbon dioxide. However, carbon neutrality is now a global objective for all nations. Consequently, energy shortages and environmental contamination make energy conservation and a  $CO_2$  reduction two of the most crucial global issues (Makoto et al., 2008). Numerous techniques for conserving conventional energy have been developed, such as utilizing renewable energy and increasing energy utilization efficiency. Solar energy is one of the most significant renewable energy technologies due to its accessibility, safety, and affordability. It has been utilized in construction and industry for heating, electricity generation, etc (Wang et al., 2020). Due to its inconsistency and sporadic functionality, solar energy is unsuitable for certain applications under particular circumstances. Therefore, in order to improve its stability and efficacy, it is combined with other technologies. The heat pump is an excellent technology for connecting with solar energy directly or by utilizing a conduit to connect with other renewable energies, such as air sources, ground sources, and water sources.

Thermal solar energy, photovoltaic solar energy systems, and heat pump systems for cooling and heating are becoming more widespread. Between 2010 and 2017, the supply of energy from solar panels increased by more than 13 times (from 32 GWh in 2010 to 444 GWh in 2017) (IEA, 2019). These have been studied by many people on their own, and each has its own optimum application, and system scheme. Although there are numerous studies on solar-assisted heat pumps for cooling and heating, still many aspects to investigate in order to promote the development and application of renewable energy heat pump systems, such as the optimization design and sizing in order to increase the performance of the system, as well as the optimal operation control strategies, that could aim to reduce the cost of investments, focusing more on energy storage issues that is a challenging aspect of the renewable energy systems. The aim of this work is to build a double-source solar-assisted heat pump (solar energy and ambient temperature) with a storage tank and investigate the impact of controlling the inlet temperature over three days, by comparing the results of the outlet temperature of the solar collector in the same solar irradiation condition in each of three days. Therefore, my hypothesis is that the lower the temperature of the heat transfer medium entering the collector, the higher the collector's performance will be, then more extracted heat will be gained to assist the heat pump evaporator, then increase the efficiency of solar energy usage and increase operating time.

The principal content of the thesis is divided into three sections. The first chapter provides a literature review of the research that encourages SAHPs' different applications, focusing on how frequently solar collectors are used as a heat source for heat pumps, as well as how those applications have been set up and under what conditions (temperatures, wind speed, and global radiation) and over what ranges. In particular, where are those different applications, highlighting the technical feasibility and economic viability of solar collectors as a heat source for heat pumps. The options and software that are available for modeling solar collectors and heat pumps and mathematical models of a solar-assisted heat pump system are also included in

the first chapter. The second chapter is under the name of Material and Methods where the description of the material used in building the system, such as the main components' position and the different sensors to measure the temperature and solar radiation instantly during the running phase of the system and the data record software used to collect and record data for fodder utilization. The last chapter is the Result and Discussion, where the obtained results are exposed and interpreted.

## **2 Literature review**

### **2.1 Introduction to literature review**

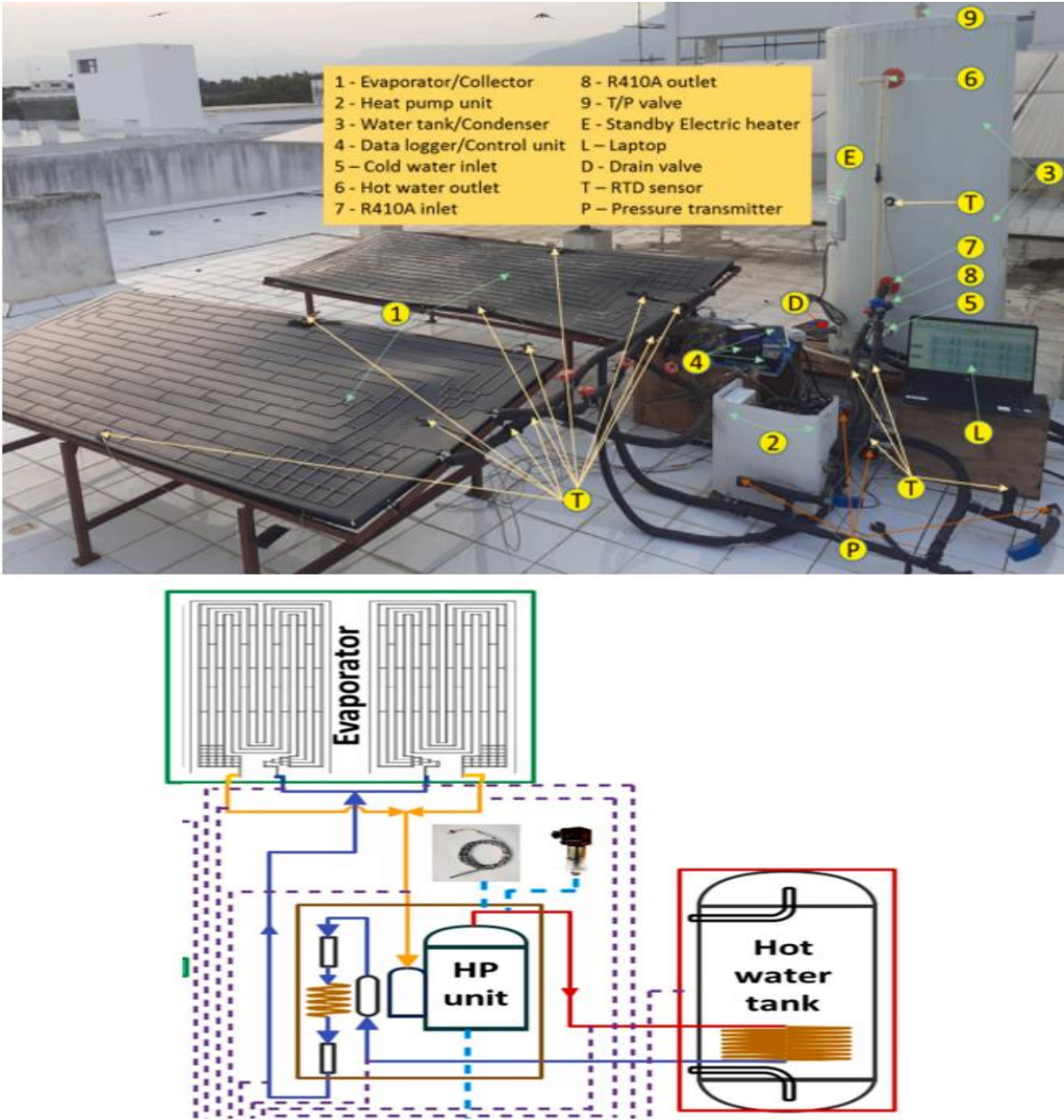
A heat pump is a device that transfers heat from one place to another, typically from a lower-temperature source to a higher-temperature sink. by using a refrigerant, which is a fluid that absorbs and releases heat as it circulates through the system. The refrigerant is compressed, which raises its temperature, and then passed through a condenser where it releases heat to the surrounding environment (Space heating, Hot water preparation). The refrigerant is then expanded, which lowers its temperature, and passed again through another heat exchanger where it absorbs heat from the source. The heat pump has the ability to use renewable energy sources, such as solar, which makes them an appropriate heat and electricity source for heat pump systems. A solar-assisted heat pump (SAHP) system has been shown to significantly reduce electricity use and increase the use of renewable energy for domestic heating (Cai et al., 2019). As solar energy can be used to power a heat pump's compressor using photovoltaic (PV) electricity or combined with ground- or air-source heat exchangers to enhance performance, it is said that solar thermal heat pumps are the most extensively researched and economically viable type (Wang et al., 2020).

Solar-assisted heat pump (SHP) systems can be divided into direct-expansion and indirect-expansion heat pump kinds based on the system structure (Yerdesh et al., 2020) (Si et al., 2015).

### **2.2 Direct expansion solar-air source heat pump system**

The direct-expansion solar-assisted heat pump (DESHP) was first proposed by Sporn and Ambrose in 1955 (Sporn., 1955). The DESHP, in contrast to traditional heat pumps, uses the solar collector as the heat pump's evaporator. The refrigerant then is circulated directly through the outdoor solar collector. For improved experimental results, Li and Yang. (2010) investigated the viability and performance of parallel evaporators in direct expansion solar-assisted air source heat pumps (DESHP). For building heating applications, Liang et al. (2011) suggested a DESHP with flexible operational modes that has a heating capacity of 10 kW for various solar collector areas. Deng and Yu. (2016) used electronic expansion valves for each evaporator to replicate the DESHP 's performance with parallel connections of the solar and air evaporators. It was discovered that when compared to single-source heat pumps, the DESHP 's heating time is reduced by 19.8% and its COP is raised by 14.1%. Experimental research on the temperature efficiency of air source heat pumps AHP, DESHP, and direct expansion solar air source heat pumps (DESAHP) was conducted by Liu et al. (2016). The dual-source DESAHP has a COP (coefficient of performance) that is 59% greater than that of single-source heat pumps, according to the results. When using phase change materials, DESAHP was experimentally

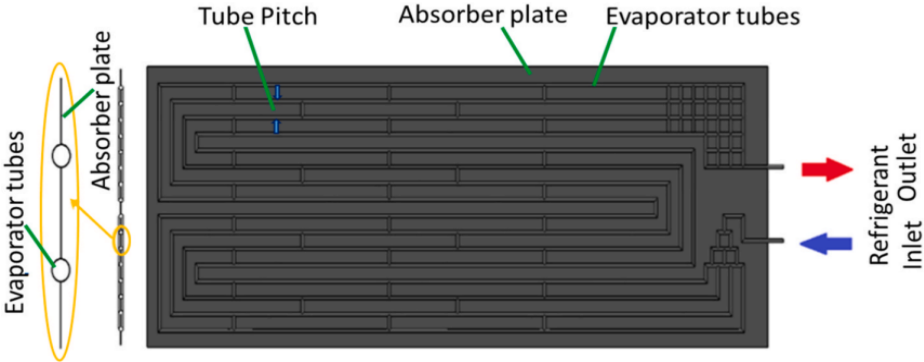
investigated by Ni et al. (2016) for both, the cooling and heating phases. The suggested system's average COP was determined to be 2.8 and its thermal capacity to be 5.6 kW. The dynamic behavior of the DESAHP was examined by Cai et al. (2019) at three distinct arrangements of air and solar evaporators connected in series and parallel. The configuration of the solar-air parallel heat pump was determined to have the greatest COP, standing at 4.8. In a water heating system using cascade storage tanks and a control strategy method, Wang et al. (2020) performed a thermal performance study of a solar collector incorporated AHP-DX and found that the yearly energy consumption could be decreased by 26%. The performance of DESAHP for dual-source absorption has been extensively studied. To clarify the direct expansion solar-assisted heat pump, I am going to use Chinnasamy et al. (2023)'s example, where the research is more focused on adapting a dual-source evaporator to capture thermal and solar energy in both heating modes (solar air mode: SAM, air mode: AM) throughout the day.



**Figure 1.** Installation layout of DESAHP system (Chinnasamy et al., 2023)

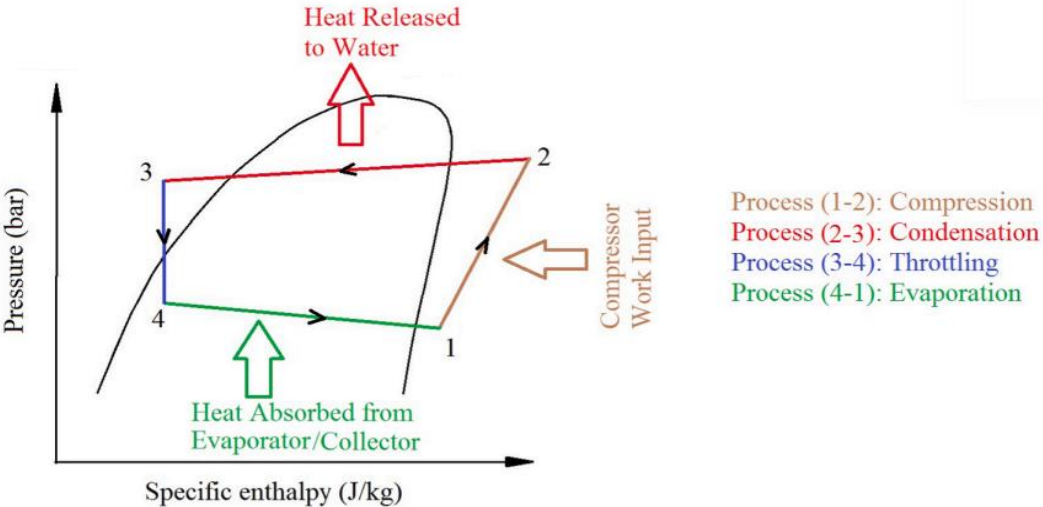


Figure 1 shows the suggested experimental DESAHP system's schematic execution configuration for supplying hot water. An expansion valve, rotating hermetic compressor, water-cooled condenser with a hot water storage tank, and dual-source plate evaporator make up the majority of the DESAHP system. The extraction of both the solar energy and air heat source is accomplished using a dual-source plate evaporator, as shown in Figure 2.



**Figure 2.** Schematic of the dual-source evaporator (Chinnasamy et al., 2023)

The primary component of this dual-source plate evaporator is an unglazed solar roll-bond bare plate collector. The anodized aluminum sheets are covered in a selective solar absorptive covering. Through the roll bond, two metal slabs and aluminum tubes are combined. The condenser is mounted on the building's rooftop at the same angle same as the latitude ( $11.5^\circ$  N) of the location of the experiment. The R410A vapor refrigerant is compressed using an 870 W rotating hermetic compressor with a displacement capacity of  $10.9 \text{ cm}^3$ . An insulated hot water storage tank is used as a condenser to exchange the heat energy from the R410A vapor refrigerant to the water. The hot water storage tank is surrounded by copper tubes that contain refrigerant and act as a condenser. On both summer and winter days, the tank is filled with 300 L of water which is heated up to  $55^\circ\text{C}$  on both the summer and winter days. (Chinnasamy et al., 2023).



**Figure 3.** Working principle of SAHP-DX system (Chinnasamy et al., 2023)

Chinnasamy et al. (2023) Found after the evaluation and comparison of the system's performance of direct expansion solar air source heat pump system (DESAHP) in SAM (solar and air mode) and AM (air mode) operating with R410A, in both summer and winter that COP of the DESAHP -SAM system varies during the sunny hours from 5.1 to 2.6, with an average value of 3.5. While the COP of the DESAHP -AM system varies from 4.1 to 2.2 with an average value of 3.0 during the night and in the lack of radiation, because DESAHP -SAM's daily average COP is greater than DESAHP -AM's, the system can run on less power. In addition, the DESAHP -SAM system requires between 155 and 199 minutes to heat water from 31 degrees Celsius to 50 degrees Celsius, with 165 minutes being the average. While the DESAHP -AM system's heating time varies from 205 to 225 minutes, with an average of 216 minutes. Moreover, the COP of DESAHP in SAM and AM modes decline with regard to tank temperature. In relation to the rise in tank temperature, system Condense capacity and power consumption decline for the corresponding heating mode.

#### *2.2.1.1 Indirect expansion solar-assisted heat pump*

In an Indirect expansion solar-assisted heat pump (IDESHP), the solar collection transmits heat to water that is circulated either through the heat pump's evaporator or through the heat exchanger inside the thermal energy storage (TES) tank, therefore the refrigerant, in this case, is not circulating through the solar collector. IDESHHP has been used extensively for producing hot water (Sterling et al.,2012), space heating (Emmi et al.,2015), cooling spaces (Nouri et al., 2019), and drying (Wang et al., 2019). In addition to the working conditions, such as solar radiation and temperature, the IDESHHP's efficiency is also influenced by the energy source. According to the different energy sources, the IDESHHP system can be classified into a single source SHP system (IDESSHP) (Bai et al.,2012), solar-assisted ground source heat pump system (IDSGHP) (Si et al.,2014), solar-assisted air source heat pump system (IDESAHP) (Jinping et al., 2022), solar-assisted water source heat pump system (IDSWHP) (Sezen et al., 2021).

These energy sources have a high energy capacity, allowing the heat pump to work at a high coefficient of performance, resolving the issue of providing poor amount and quality of energy for a building or other industry and accomplishing multi-energy delivery, including power, space heating, cooling, and drying (Zhou et al., 2022). These IDESHHP systems each have unique characteristics and various purposes. With the benefits of a broad range of energy sources, consistent operation, commercialization, ease of installation and maintenance, high energy efficiency, and COP (Zhou et al., 2022).

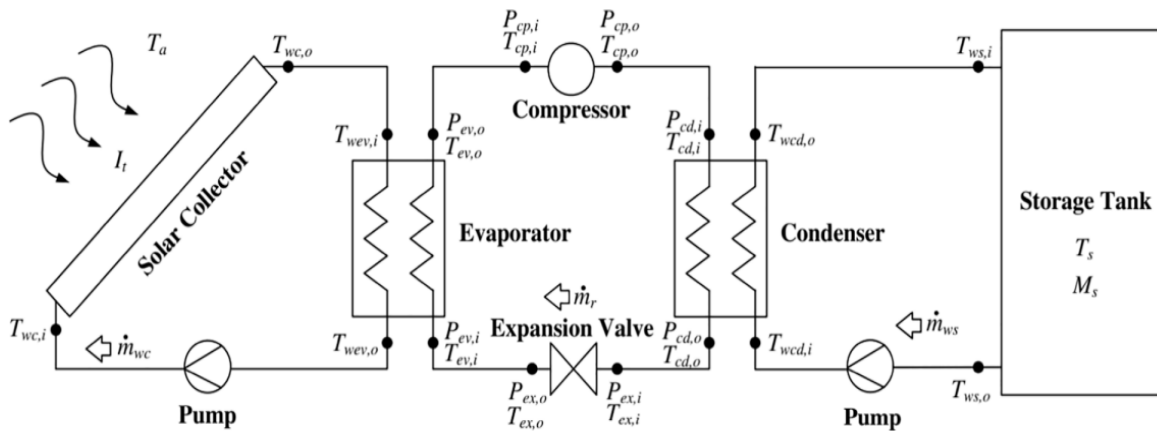


**Figure 4.** Schematic diagram of a solar-assisted heat pump system (Nuntaphan et al., 2009)

### 2.2.2 Indirect expansion single-source solar-assisted heat pump system

An IDESSHP system only uses solar energy as the energy source. The condenser of the heat pump is attached to the water reservoir, and the solar collector is connected to the heat pump's evaporator. As soon as the system is running, the solar collector takes in sunlight and transforms it into thermal energy. The working liquid fluid then transports this energy into the evaporator, where it is absorbed by the refrigerant in the heat pump. A compressor increases the temperature of the refrigerant and its absorbed energy which is then released and kept in a storage tank for later use as domestic hot water or space heating. In IDESSHP devices, water is typically used as the working fluid to transport thermal energy from a solar collector to the heat pump. Dikici et al. (2008) connected the heat pump's evaporator and solar collection directly, and the testing findings revealed that the system's COP is 3.08. The energy storage tank is added to the system to increase the efficiency of solar energy usage and increase operating time. Bakirci et al. (2011) linked the solar collector, evaporator, and water tank all in parallel. The experiment conducted from January to June revealed that the solar collector's COP varied from 3.3 to 3.8 and its thermal efficiency ranged from 38% to 60%.

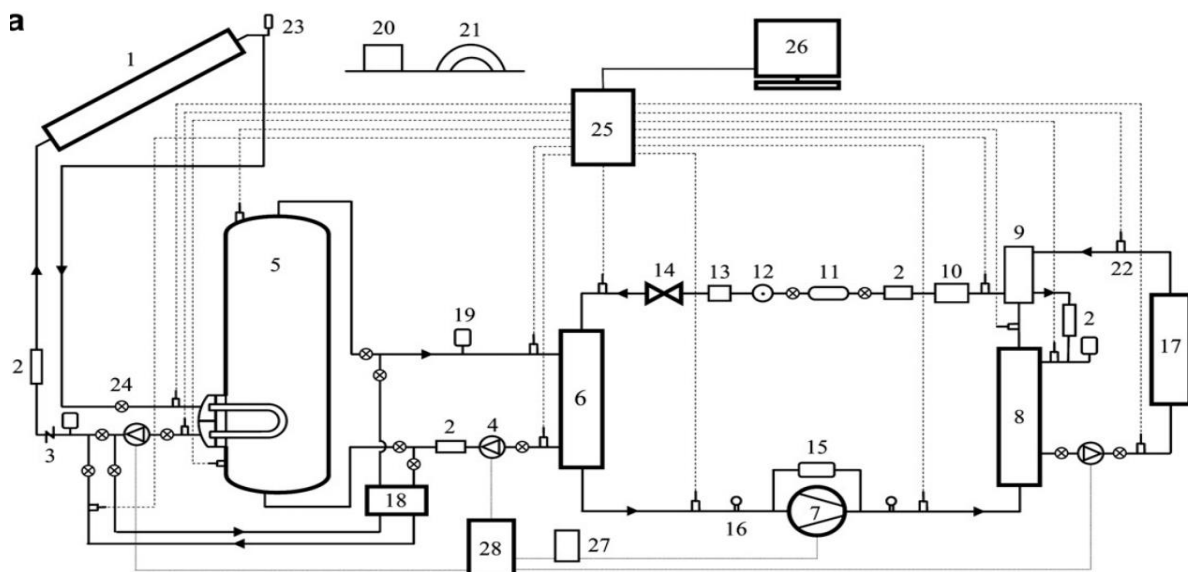


**Figure 5.** Schematic representation of the parallel system (Bakirci et al., 2011)

1. Solar collector
2. Flow meter
3. Check valve
4. Circulating pump
5. Energy storage tank
6. Evaporator
7. Compressor
8. Condenser
9. Prior heating and sub-cooling exchanger
10. Receiver
11. Dryer
12. Sight glass
13. Selenoid valve
14. Expansion valve
15. Pressure gauge
16. Manometer
17. Radiator
18. Plate-heat exchanger
19. Expansion tank
20. Integrator
21. Pyranometer
22. Thermocouple space
23. Air outlet pipe
24. Valve
25. Data acquisition card
26. Computer and monitor
27. Electronic counter
28. Control panel

Yumrutas et al. (2004) linked the solar collector, water tank, and evaporator all in series and the testing results showed that its COP varies between 2.5 and 3.5 under the climatic circumstances of Turkey's southern area.

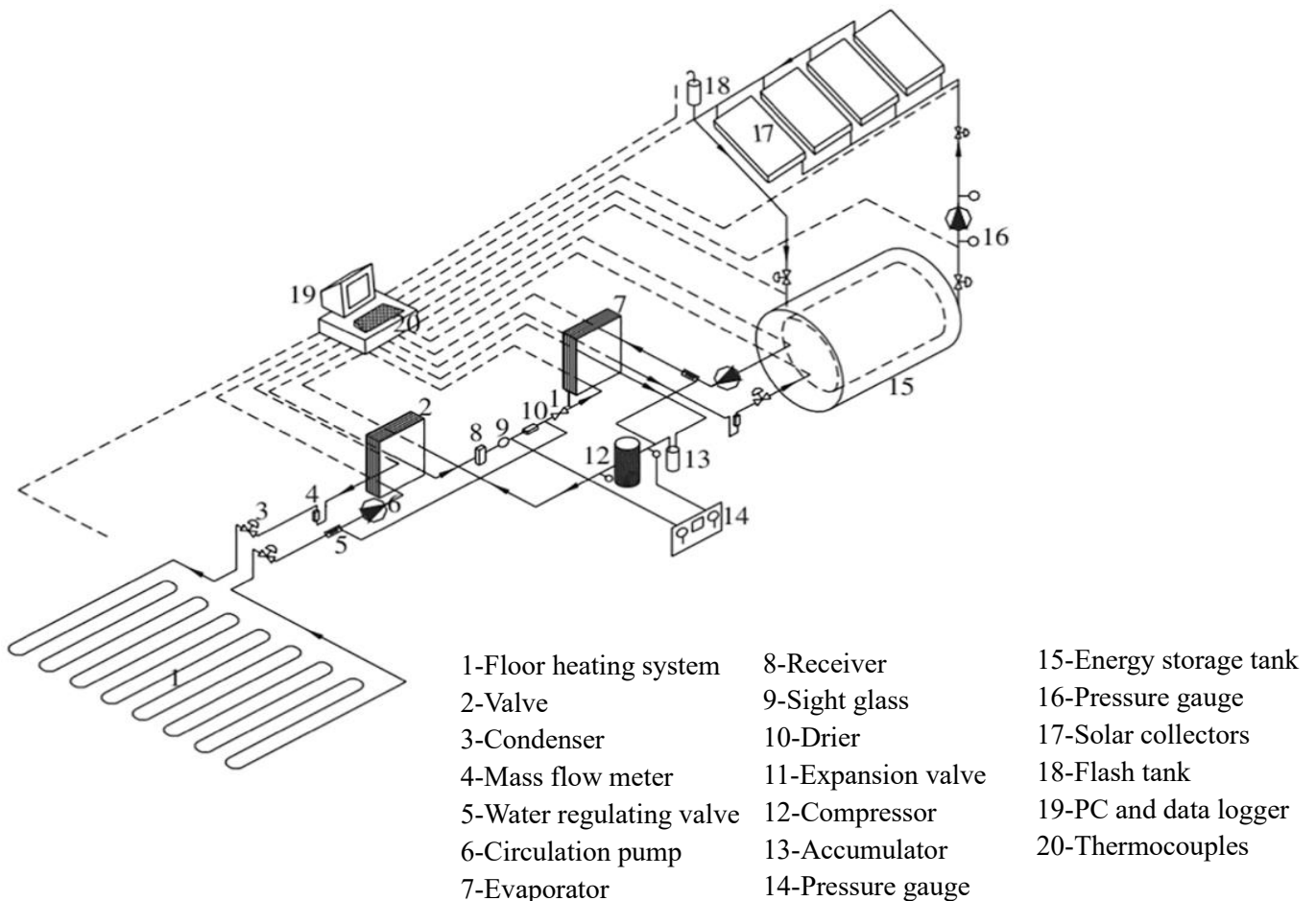


**Figure 6.** Schematic representation of the series system (Yumrutas et al., 2004)

The evaporator and water reservoir were composed together by (Ahmet et al., 2012). The evacuated tube solar collector's efficiency ranges from 0.807 to 0.728, and the highest measured COP is 6.38.

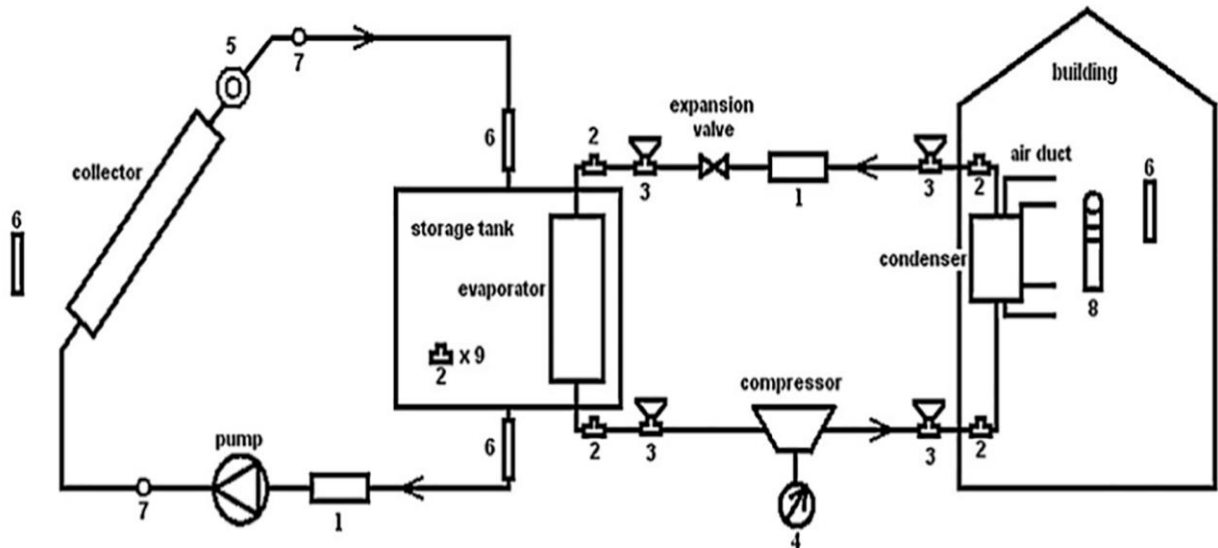


**Figure 7.** Schematic representation of the combined system (Yumrutas et al., 2004)

- |                          |                      |
|--------------------------|----------------------|
| 1. Rotometer (flowmeter) | 5. Pyranometer       |
| 2. Thermocouple          | 6. Glass thermometer |
| 3. Pressure transducer   | 7. Thermometer gage  |
| 4. Wattmeter             | 8. Thermoanemometer  |

Dannemand et al. (2020) used two water containers to gather the low and high-temperature energy from solar collectors and heat pumps in order to make better use of the solar energy temperature difference. Additionally, it was discovered that from October to January, the PV/T collector transmitted 0.4 kWh/m<sup>2</sup> per day of heat to the storage tank, acting as an absorber in cold conditions (Figure 8).

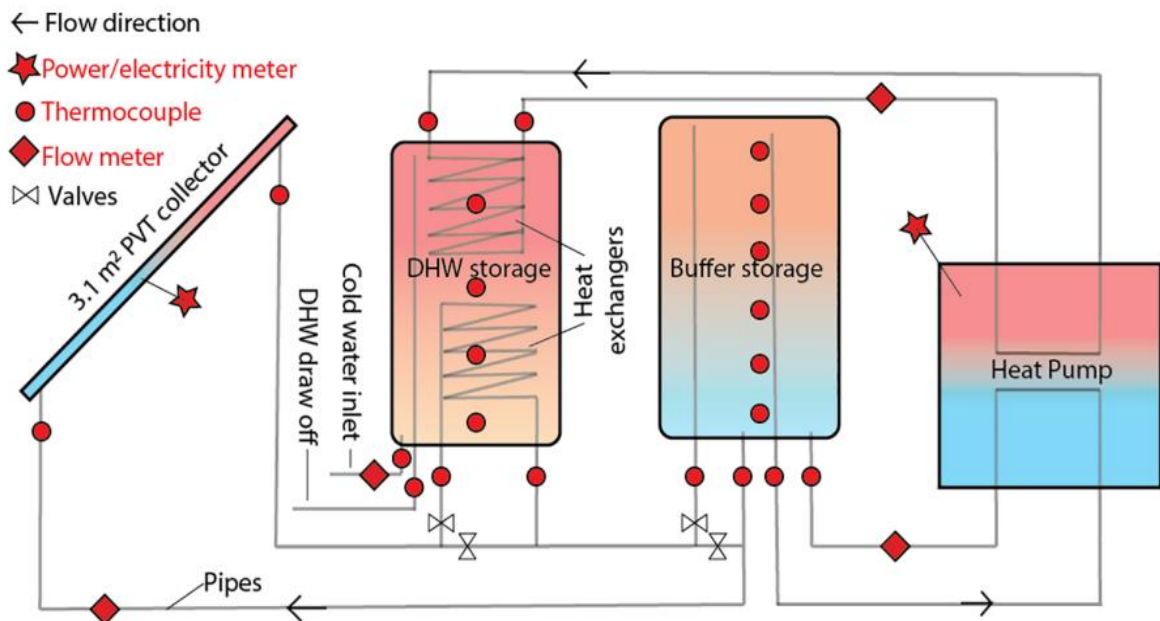


**Figure 8.** Illustration of the solar-assisted heat pump system with two tanks (Dannemand et al., 2020)

The domestic hot water (DHW) storage tank was connected to the thermal absorber of the PVT collector by the heat exchanger spiral in its bottom. Additionally, with a straight inlet to the top of the tank the 200 L buffer storage tank, was connected to the solar collector. A heat exchanger located at the top of the DHW tank storage connected the tank with the heat pump as an additional heat source. The heat pump was turned on when the solar collector's heat wasn't enough to keep the top of the DHW tank at the desired temperature. The heat source of the heat pump in this case is the buffer storage tank. The solar collector loop and buffer storage were filled with a propylene glycol/water solution at a 40% concentration. The thermal power production reaches a 3.15 kW at 0/35 °C (0 °C at the input on the source side of the heat pump, 35 °C at the output on the load side of the heat pump), and a 0.67 kW (electrical) electrical power usage with COP 4.70 (Dannemand et al.,2020). A PV/T module was selected as the energy source by Dannemand et al. (2020) because it has the advantages of versatility and high efficiency. Theoretical findings indicated that the capacity of the water tank, the quantity of PV/T modules, and the buffer all had a significant impact on the performance of the solar heat pump system. Amo et al. (2019) inserted four water containers into the SSIDESHP system by the two containers on the evaporator side are used to gather water from the solar collector at various temperatures, while the two other tanks on the condenser side are used for cooling and heating. As a consequence of the working fluid temperature fluctuation, the yearly COP varies from 2.96 to 4.26, and PV/T could supply 67.6% of the heat pump's required energy. The PV/T and evaporator were connected using a heat pipe by (Zhang et al., 2013) and the test results showed that the PV/LHP module's mean daily electrical, thermal, overall energetic, and energetic efficiencies were measured at 9.13%, 39.25%, 48.37%, and 15.02%, respectively. 5.51 was recorded as the coefficient of performance of the system.

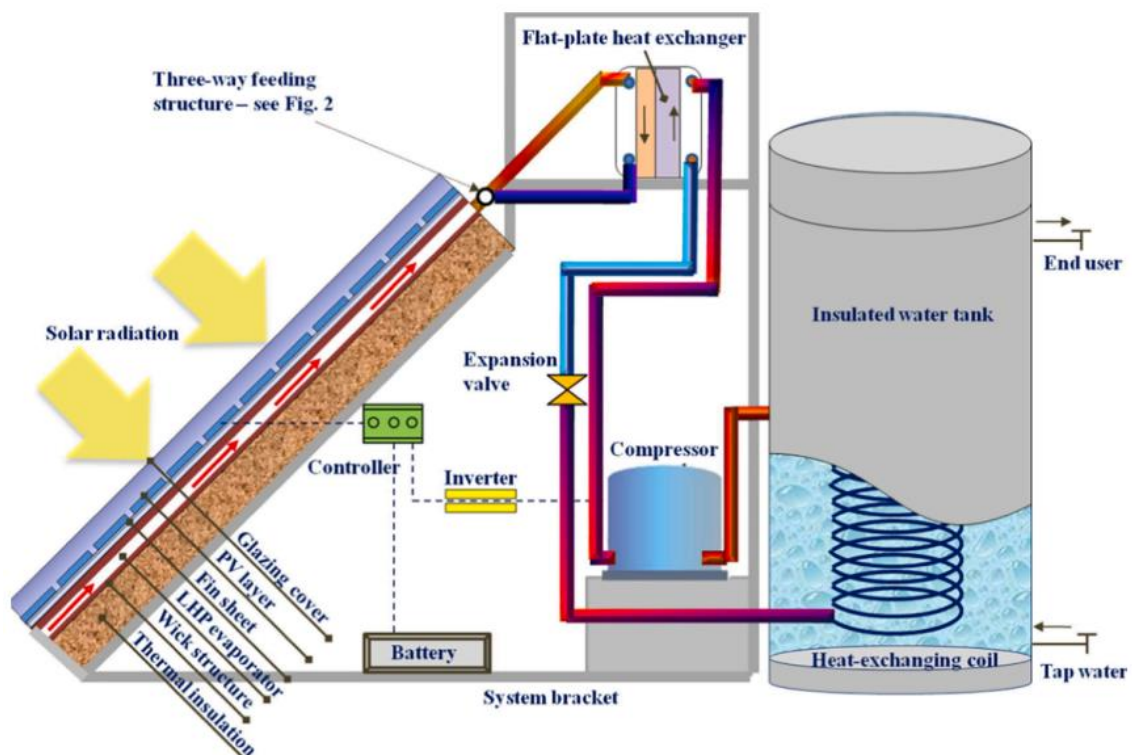


**Figure 9.** Schematic design of the solar PV/LHP module-based heat-pump water heating system.

(Zhang et al., 2013)



Phase change material (PCM), is also presented as one of the heat storage techniques and has the benefits of high latent heat storage capacity, isothermal phase transition, and high energy density. The phase change in heat storage capacity is around 3-11 times that of the sensible heat capacity of widely known materials (Khan et al., 2016). The heat storage units in DHW are commonly used to supply instant hot water using sensible heating. Thus, the heat capacity depends on the volume of the tank. Phase change materials (PCM) may be an answer to this volume problem. Due to their ability to store sensible and latent heat, which can result in a reduced volume for the same heat capacity storage (Kutlu et al., 2020). The performance of solar heat pump systems with and without PCM was evaluated by (Youssef et al., 2017), On sunny and cloudy days, it was discovered that the PCM increased the system's average COP by 6.1% and 14.0%, respectively. Numerous researchers have constructed models and conducted tests. These works primarily concentrate on the different PCM configurations and characteristics found in water tanks. According to an experiment conducted by Mehling et al. (2003) applying PCM to the roof of a water reservoir improves holding capacity and offsets thermal losses. In a modeling analysis of PCM with water storage. Talmatsky et al. (2008) examined the performance taking DHW demands into account. They came to the conclusion that using PCM does not significantly improve energy efficiency, and they provided an explanation of how rewarming water by PCM at night increases losses to the environment. The same mathematical model as Talmatsky et al. (2008)'s one, was also taken into consideration by Kousksou et al. (2011) who also created a water tank model with a solar collector, a PCM, and a supplemental heater. They stated that the chosen PCM melting temperature has a significant impact on energy efficiency, so thorough consideration of the design parameters is advised. On the contrary, Kutlu et al. (2020) proposed the use of subcooled PCMs, Sodium acetate was chosen as the thermal storage material because of its comparatively stable state at the supercooled condition and the appropriate freezing temperature of 58 °C, which can provide promising hot water supply for homes. The proposed system's primary goal is to use supercooled PCM tubes inside the water tank to increase the system's heating capacity and, more specifically, its energy efficiency. As can be seen in Figure 10, cylindrical PCM tubes are placed at the top of the water tank. To take advantage of the water tank's thermocline behavior.

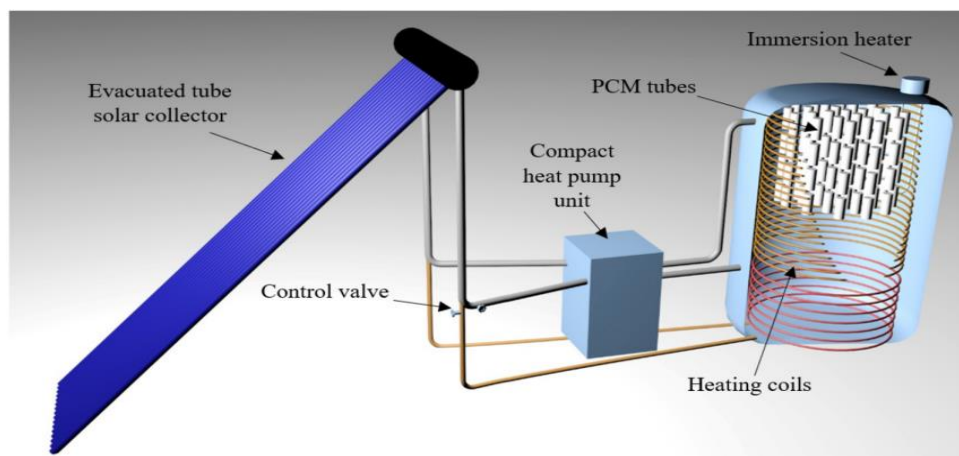


**Figure 10.** Solar-assisted heat pump hot water system with a PCM-integrated water tank (Kutlu et al., 2020)

The system operates in various phases. Four components make up the solar-assisted heat pump. The solar collector is the first component, evacuated tube heat pipe collectors are chosen Due to their excellent performance even in low ambient temperature conditions, to heat the circulating water. Heated water by the collectors is either used as a heat source for the heat pump or for the heating circuit in the water tank. The second component is the heat pump unit, it is a water source heat pump unit that boosts the sun heat that has been captured by the heated water and raises the tank temperature until the top temperature hits the desired level. The third component is a water tank, which is typical of homes. For the purpose of giving the residents heated water. Finally, a temporary domestic load profile is modeled in order to assess the system's efficiency in actual usage (Kutlu et al., 2020).

Kutlu et al. (2020) Come to that in various volumetric proportions of water and PCM in the storage tank, an improvement in energy storage capability can be observed. The results are presented in Table 1. Energy storing capacity for various PCM substitution replacement with water are shown when the tank temperature drops from 70 °C to - 40 °C. For 200 L of water, the total heat storage energy is 25.2 MJ, but when 10% of the total volume changed with the PCM, the total heat storage capacity increases to 32.76 MJ. The overall heat storage capacity of the reservoir is nearly 30% higher when even 10% of the water is substituted with PCM material.

**Table 1.** Energy storage capacities of DHW tank (Kutlu et al., 2020)

| 200 L tank | PCM         |               |           | Water         |           | Tank (40 °C–70 °C) |           |
|------------|-------------|---------------|-----------|---------------|-----------|--------------------|-----------|
|            | Latent heat | Sensible heat | Mass (kg) | Sensible heat | Mass (kg) | Storage capacity   | Mass (kg) |
| Water only | –           | –             | –         | 25.2          | 200       | 25.2 MJ            | 200       |
| 5% PCM     | 3.8         | 1.24          | 15.2      | 23.94         | 190       | 28.98 MJ           | 205.2     |
| 10% PCM    | 7.6         | 2.48          | 30.4      | 22.68         | 180       | 32.76 MJ           | 210.4     |
| 20% PCM    | 15.2        | 4.95          | 60.8      | 20.16         | 160       | 40.32 MJ           | 220.8     |
| 30% PCM    | 22.8        | 7.44          | 91.2      | 17.64         | 140       | 47.88 MJ           | 231.2     |

Continuing with a single source-assisted heat pump, Borehole heat exchangers are currently the most efficient heat sources for heat pumps (Christian et al., 2014). Solar ice systems are an additional heat source that can take the place of using ground or ambient air sources (Daniel et al., 2018). Since ice storages are stocked with pure water, they can be placed in water protection areas as well as locations where deep drilling is either impossible or prohibited. (Christian et al., 2014). examines how well a combined solar, heat pump, and ice storage system for dwellings performs during different seasons. The mechanism of solar-ice heat generation is schematically depicted in Figure 11.



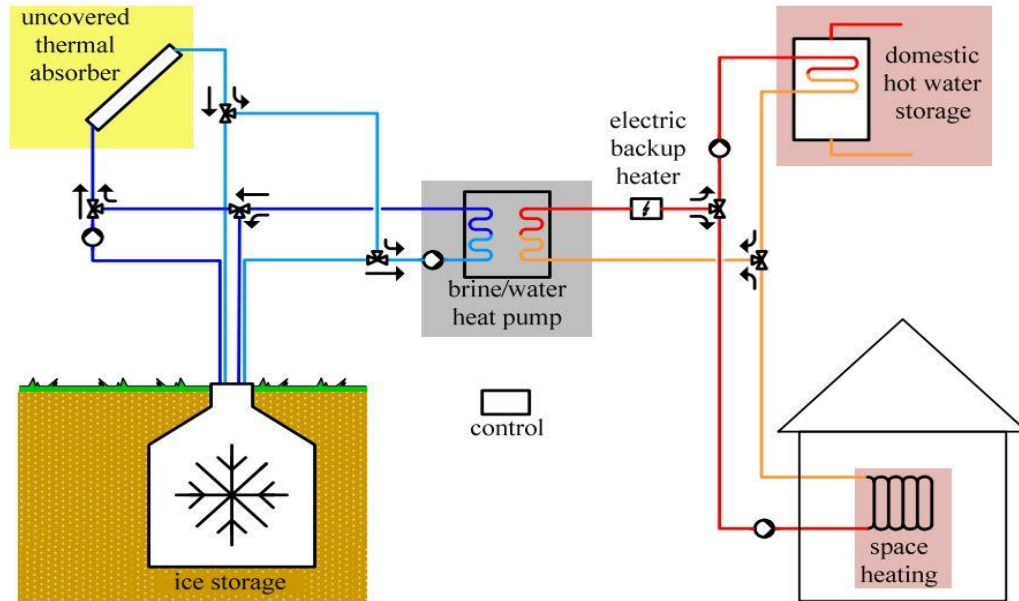


**Figure 11.** Solar-ice storage heat generation system. (Christian et al., 2014)

The main part is a brine/water heat pump that provides heat for domestic hot water (DHW) preparation as well as space heating. An unglazed solar absorber serves as the heat pump's main heat source, generating heat both from solar irradiation and convective gains. In the event that the absorber is unable to provide enough heat, buried ice storage acts as a backup heat source for the heat pump. In the phase change from water to ice, where heat is primarily held as latent heat, in the ice storage. The ice store is refilled using extra heat from the solar absorber. The ice store also absorbs heat from the surrounding soil. The temperature in the ice store quickly decreases as soon as all the water is frozen and more heat is removed. When the heat pump's source temperature falls below its operating threshold, which is typically around  $-10\text{ }^{\circ}\text{C}$ , the heat pump turns off. An electric reserve heater is then used to give heat (Christian et al., 2014).

In the intended heat-generating system, the solar absorber's primary function is to act as a heat source for the heat pump. and the excess heat is stored in the ice storage. The ice storage and the heat pump only require a temperature below  $20\text{ }^{\circ}\text{C}$ . Therefore, an unglazed solar collector is used. The benefit of an unglazed collector is that, if the working temperature of the absorber is below ambient temperature, both solar energy but also the enthalpy of ambient air via convection can be used as heat sources. Even heat gains from condensation can be used in some circumstances when the temperature of at least portions of the absorption surface is below the dew point temperature (Christian et al., 2014). Ice storage is an underground heat source for a heat pump. Until all of the water inside has frozen into ice, heat can be successfully removed and extracted from the ice store. The supply temperature to the heat pump is always close to the freezing point because the temperature is unaffected when a substance transitions from a liquid to a solid state. The freezing process is interrupted by phases of renewal, where heat is added to the ice store from solar absorbers or the surrounding soil as the ice storage is not insulated. The solar absorbers can be used for renewal at low ambient temperatures due to the low temperature in the ice store. During the hot summer months, the ice in the ice storage fully melts and the water is heated to about  $25\text{ }^{\circ}\text{C}$  when little energy is required for SH and solar heat is abundant. As a result, the ice store serves as a seasonal warming source (Christian et al.,

2014). Christian et al. (2014) found that A significant quantity of heat can be removed by freezing the stored water; for every kilogram of water, this procedure releases 333 kJ (0.093 kWh). Compared to that, 4.19 kJ/(kg K) or 0.001 kWh/(kg K) can be recovered using the sensible heat of water at temperatures above 0 °C. From these figures, it can be surmised that freezing 1 kg of water released the same amount of heat that can be extracted by cooling 1 kg of water from approximately 80 °C to 0 °C (Christian et al., 2014).

It is possible to use a variety of heat exchanger designs for the latent heat from ice storage. (Daniel et al., 2018). Each concept must make sure that the ice coating on the particular heat exchanger does not get too thick for the concept and does not cause the source temperature for the heat pump to get too low. There are essentially two approaches to designing heat exchangers for ice storage:

- (a) A large heat exchanger surface evenly spread throughout the entire storage volume. A maximum ice coating thickness of several centimeters to a few decimeters is typically permitted, depending on the heat pump's extraction capacity and the specifications of the heat exchanger. The spread of the heat exchanger in the storage volume is determined by this maximal ice thickness (Daniel et al., 2018).
- (b) A small heat exchanger inside or outside of a storage space that actively removes ice from its surface or prevents it from forming (Daniel et al., 2018).

From the aforementioned systems, only the uniformly dispersed concepts are proven in the solar and heat pump heating industry (Daniel et al., 2018). The efficiency of frequently used heat exchangers for ice storage is compared based on laboratory experiments (Daniel et al., 2018).

The majority of ice-storing tanks on the market were created for cooling purposes and do not satisfy the unique requirements of solar-ice heating systems. Only a few different ice storage styles are offered, and there aren't many ice storage makers. Due to their shape and height, some of the ice storage used in solar-ice systems must be placed outside of the structure, making them only useful for single-family homes. Furthermore, the lifetime of ice storage is only assured to be 10 years, whereas the lifetime of heating systems, should be at least 20 to 25 years. Greater efficiency can be attained by expanding the area, and the number of heat exchangers placed inside the ice storage tank (Daniel et al., 2018).

In order to obtain bigger overall ice storage amounts as required, Daniel et al. (2018) designed cylindrical ice storage Figure 12. The tank's main components like heat exchangers, cylindrical vessels, fixtures, fittings, and pipes are made of stainless steel, ensuring extended service life and preventing air from leaking into the briny cycle. An overview of the storage's key characteristics is provided in Table 2.

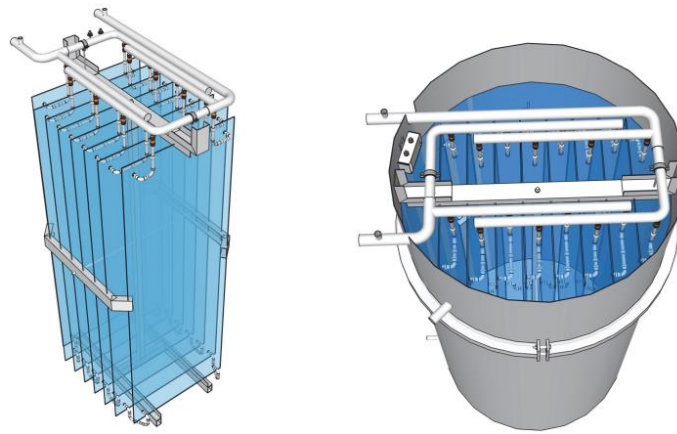


**Figure 12.** Drawing of (a) the ICESOL heat exchanger with eight heat exchanger plates made of stainless steel (transparency in the drawing as an artifact) and (b) the ICESOL ice storage with the heat exchanger immersed into the storage water.

**Table 2.** Main specifications of the ice storage as tested in the lab.

|                                       |                |      |
|---------------------------------------|----------------|------|
| Water content                         | m <sup>3</sup> | 1.97 |
| The active surface of heat exchangers | m <sup>2</sup> | 21.7 |
| Diameter of storage                   | Mm             | 1200 |
| Number of parallel pairs of hx-plates | -----          | 4    |
| Height of storage                     | Mm             | 1950 |
| Latent heat (max.)                    | kWh            | 129  |
| Maximum icing fraction                | Of mass        | 90 % |
| Distance between plates               | Mm             | 120  |

### 2.2.3 Indirect expansion double-source solar-assisted heat pump system

#### 2.2.3.1 solar assisted air-source heat pump system

The inclusion of an air-cooled evaporator in the heat pump distinguishes the IDESAHP system from the IDESHP system, thus an IDESAHP system is a system that uses solar energy and air as the energy source to provide thermal energy to the user both an autonomous solar energy system and a heat pump system is possible (Zhou et al., 2022). The solar collector and air source heat pump system are connected to the water tank in parallel, as shown in Figure 13 (Panaras et al., 2014). The solar collector takes in the sun's energy and transforms it into thermal energy, which the water pump then transfers into the water tank. Additionally, the heat pump's evaporator collects energy from the air, and the compressor warms the low-temperature energy. The high-temperature energy then dissipates into the condenser's water tank (Zhou et al., 2022).

A heat pump system using a PV/T and an air-water heat exchanger was employed by Wanget al. (2018) to provide room heating. The experimental findings showed that the COP of the PV/T-WSHP heating mode and the PV/T-W and ASHP heating mode, respectively, were 3.18 and 2.53. Under typical conditions, the unit heat capacity and COP got up to 20.1% and 20%, respectively, whereas under low-temperature conditions, they grew to 27.6% and 45.5%.

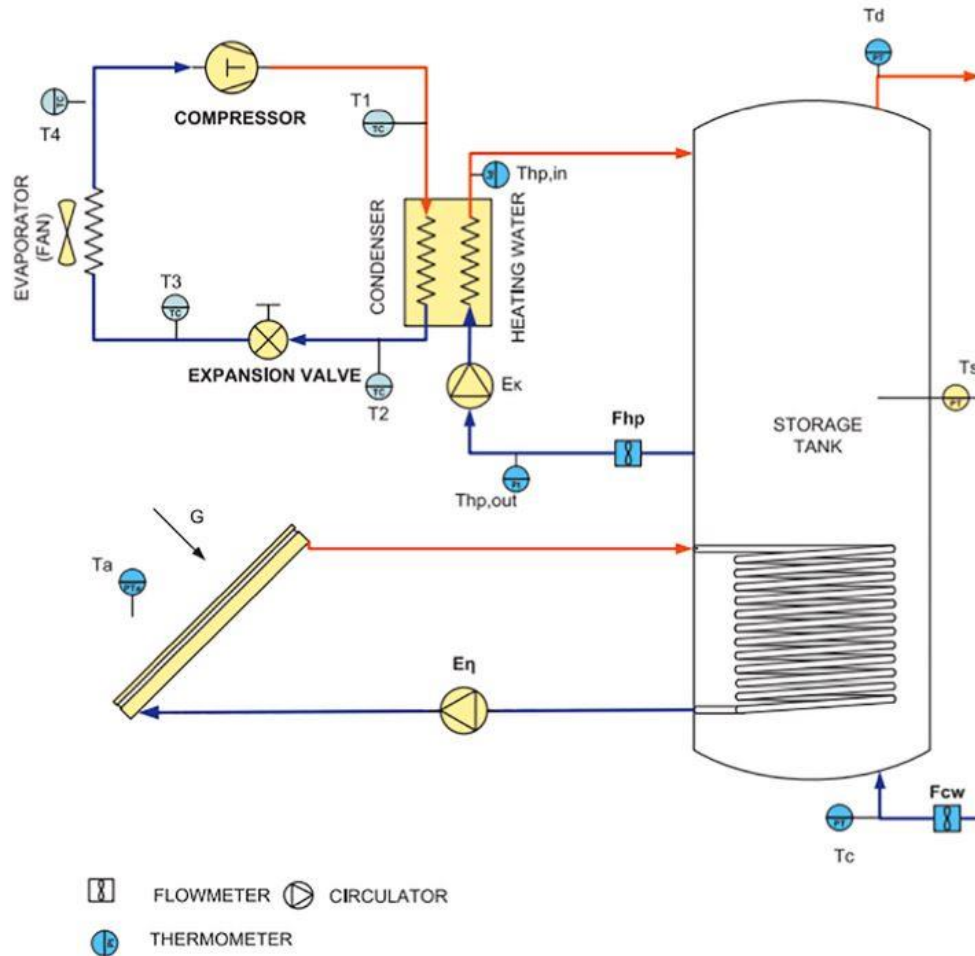


**Figure 13.** solar air-source heat pump system (Panaras et al., 2014)

Further research demonstrates that the dual heat source mode's heating capacity improves by 62% and its coefficient of performance (COP) rises by 59% when compared to the single air heat source mode (Liu et al., 2016). A unique SAHP system was presented by Cai et al. (2016) that can transition between various combinations of a heat pump's evaporator and condenser to provide varied modes and high-efficiency energy delivery. The study shows that operating a solar collector and heat pump simultaneously for the solar hot water mode is an energy-saving technique (Cai et al., 2016). To balance the heating capacity and coefficient of performance (COP) for the solar space heating mode, the mass flow of water should be adjusted in accordance with various temperature needs and heat loads (Cai et al., 2016). The research also identified the moments at which various working modes change over, and it showed that using the optimum operating strategy may result in a greater COP under all-year operation conditions (Cai et al., 2017). A novel PV/T dual source evaporator was created by Simonetti et al. (2019) who also conducted a numerical study. The results demonstrate that solar irradiation has a substantial impact on the SAHP system's performance and that this system has a 14% higher COP than a typical air source heat pump. Cai et al. (2019) suggested a novel SAHP system that links a finned tube evaporator and solar collector evaporator in succession, so that air and solar

energy may play complementary roles under different operating conditions. Considering the fact that these systems can efficiently use ambient air and solar heat, their heat exchanger construction is too complicated for engineering applications (Wang et al., 2022). According to (Ran et al., 2020) a water source heat pump is connected in parallel with two air source heat exchangers and solar collectors as shown in Figure 14, the simulation revealed that the system could provide 15%, 11%, and 12% of the total heat output by using Chengdu, Beijing, and Shenyang as the locations and the seasonal performance factor was 3.61, 3.27, and 2.45, respectively (Ran et al., 2020).

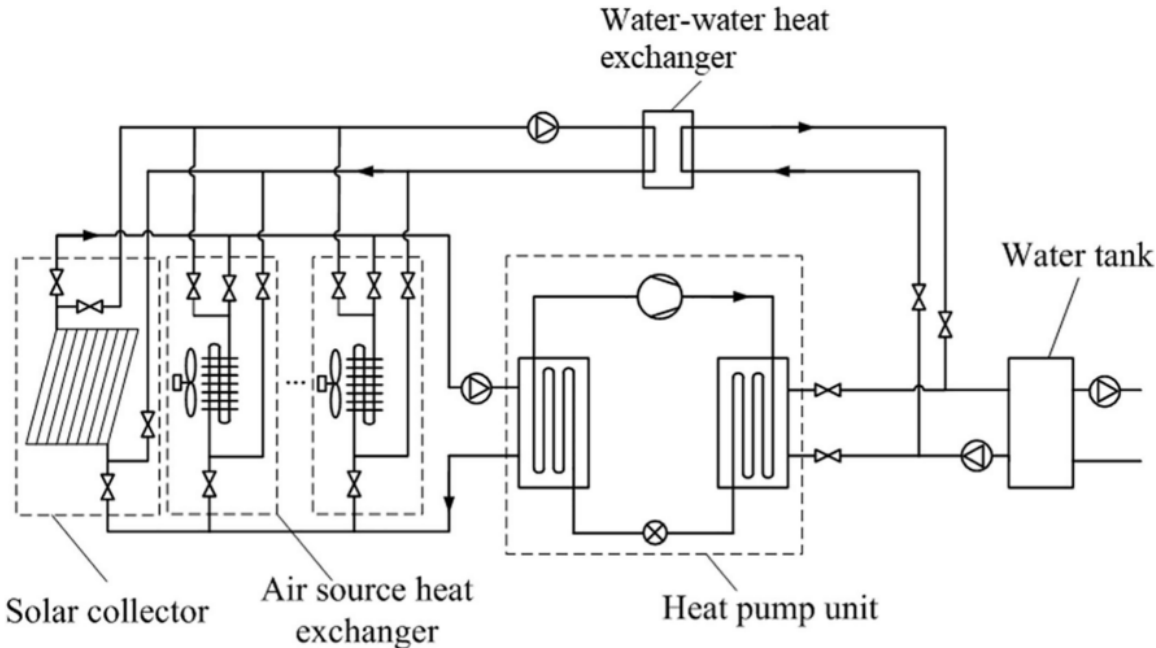


**Figure 14.** Schematic diagram of the solar-air HP system (Ran et al., 2020)

The majority of current research on the SAHP system ignores the need for energy storage during severe weather and instead emphasizes how air and solar energy complement each other. This also implies that in the persistent wintertime severe weather, the standard SAHP system cannot offer effective heating. In addition, a SAHP's practical implementation is constrained by costly system investment and complicated system structure (Wang et al., 2022). A revolutionary SAHP system, which can essentially be unaffected by severe weather and maintain a steady and efficient operation of the system, was presented by Wang et al. (2022) to make up for the insufficient heating capacity of a typical heat pump system in cold regions of North China.

The key innovation of Wang et al., (2022)'s study. is dual usage of the ice tank in winter and summer, which works in conjunction with air and solar energy to guarantee the system operates steadily and effectively in bad weather. The system structure, on the other hand, is not too complicated in terms of the heat exchange mechanism. In order to protect the system from changes in the outer environment, the system uses the condensation latent heat of the water in the ice tank as the heat source for the heat pump throughout the winter. The HSI mode's average COP was 2.35. During the day, the ice tank's heat was primarily restored using the heat collected from the PV/T module, and the air was utilized as an auxiliary heat source to ensure the system's continuous and reliable functioning (Wang et al., 2022).

For two consecutive days, the ice tank supplies the heat needed for the HSI mode in a period of poor solar irradiation during the winter. The modalities of water cold storage and ice storage bear all the cooling load of the consumers during high-temperature summer weather. According to the calculations, the SAHP system conserves 1.85 t of conventional coal annually (Wang et al., 2022).

### 2.2.3.2 solar assisted ground-source heat pump system

IDESGHP system is a system that makes use of both solar and geothermal energy. As shown in Figure 15 (Ozgener et al., 2005), the condenser is linked to the water tank or heat exchanger in the room, and the solar collector and ground heat exchanger are connected in parallel to the heat pump's evaporator. The solar collector serves as an energy source and gives the heat pump thermal energy when solar radiation is present. When solar radiation is insufficient, the ground energy serves as a source of energy and transmits heat from the surrounding soil to the heat pump's evaporator by using the working fluid in the ground heat exchanger. In the off-heating season, solar energy may also be used to energize the soil. As a consequence, the earth may both store and release energy, serving a variety of purposes throughout the year (Zhou et al., 2022).

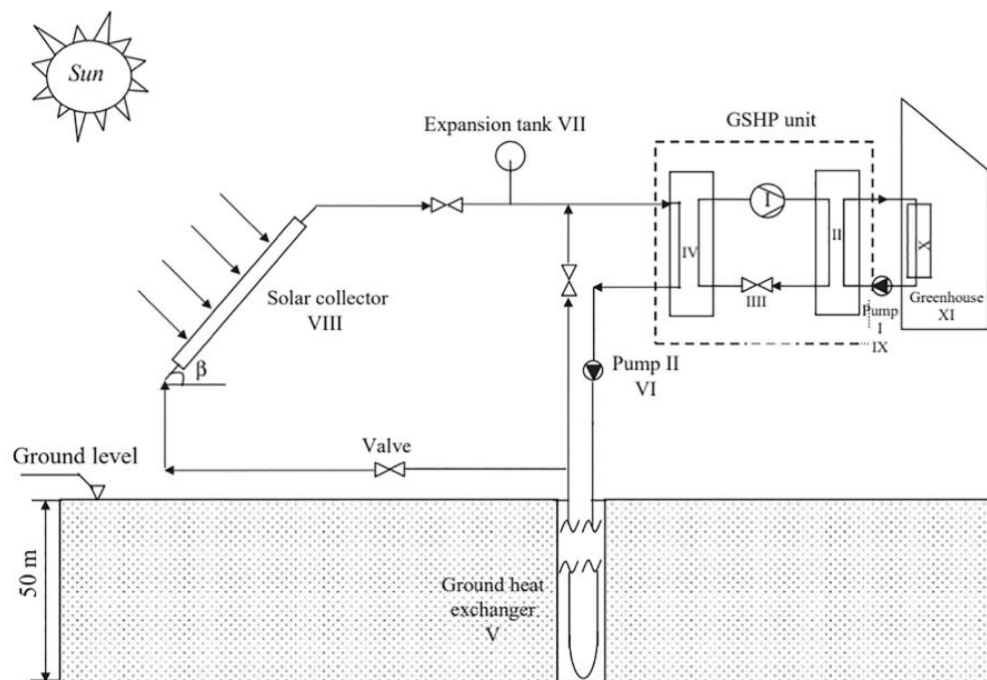


**Figure15.** The schematic of the SAGSHPS and its main components (Ozgener et al., 2005)

The solar collectors were linked to a heat exchanger by Stojanovi et al. (2010) that is in series with the GHE and evaporator. The long-term outcome showed that the heat pump's seasonal performance factor and the system as a whole were 2.85 and 2.09, respectively. (Zhou et al., 2022). The tank might be simultaneously linked to the heat pump and user terminal in order to utilize most of the varying water temperatures. The experimental average COP of the ground source and solar source operating modes, according to Yang et al., (2015), were 2.37 and 2.72, respectively. For the combined operating mode, SAHP operation mode, and solar U-tube feeding heat operation mode, respectively, the average solar collecting efficiency was 43.6%,

47.3%, and 38.8% (Zhou et al., 2022). Three tanks were assigned various purposes in the IDESGHP by Trillat-Berdal et al. (2006) as shown in Figure 16. A long-term experimentation result revealed that the domestic hot water solar percentage was more than 60%, and the heating mode COP was 3.75 (Zhou et al., 2022).

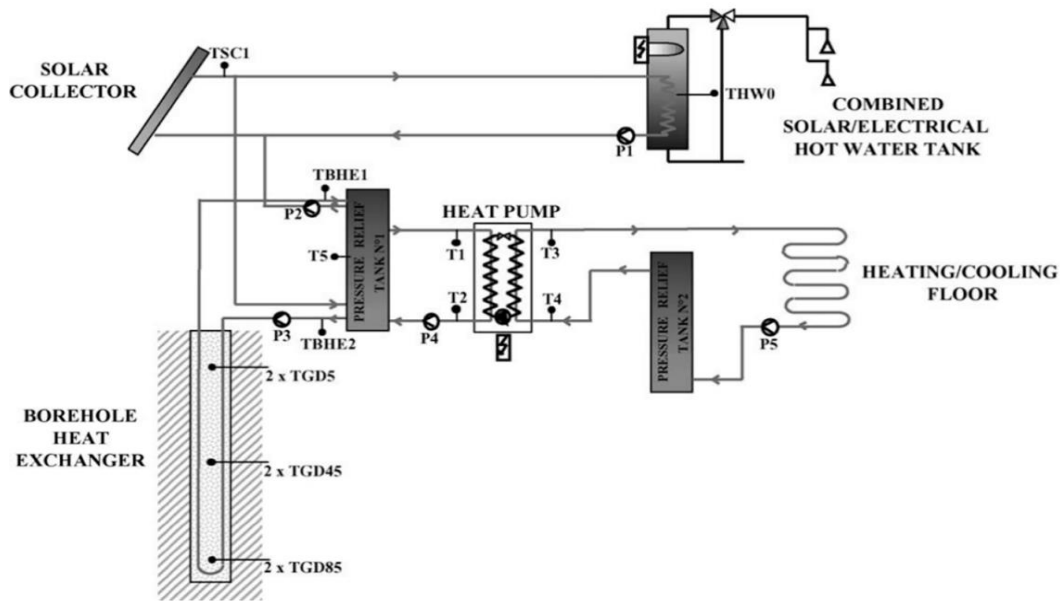


**Figure 16.** Schematic diagram of the IDESGHP system with multi tanks (Trillat-Berdal et al., 2006).

Figure 17 illustrates the two distinct HGHX-equipped supply setups that were the subject of the study by Hüsing et al. (2016) In every situation, the HGHX is implanted at a depth of 1.5 meters. Assumed to be the solar thermal supply system is an unglazed photovoltaic thermal hybrid collector (PVT). Different operating modes are possible with the hydraulic layout, including stand-alone HP/HGX mode when there are insufficient solar thermal gains, serial connection of the PVT and HGHX/HP mode when heat demand and solar thermal gains coincide, and HGHX recharging by PVT mode (at lower mass flow) when there is no heat demand at the time. Throughout the simulations, the system's condition is tracked, and a controller created for the purpose chooses the particular operating mode. To prevent overheating of the ground, the HGHX's top limit for fluid entry is 25 °C in all modes of operation (Hüsing et al., 2016)

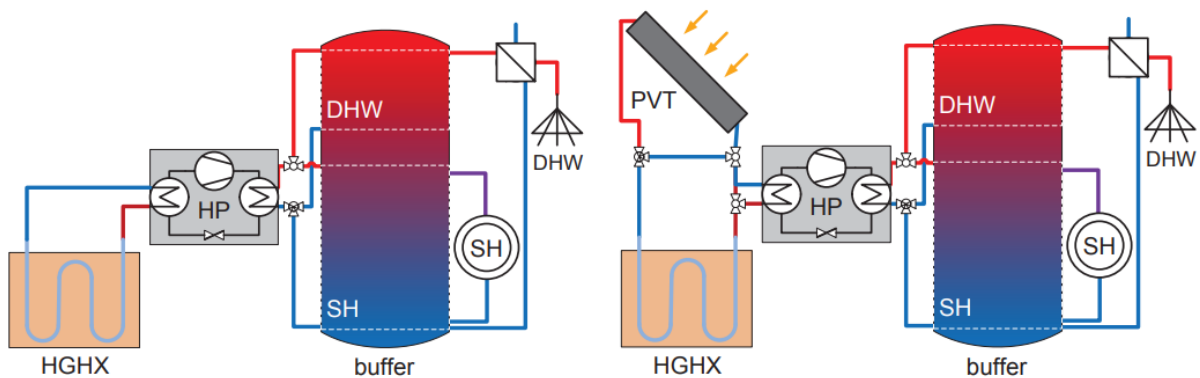


**Figure 17.** Schema of the ground source heat pump systems, with the assistance of the solar collector (Hüsing et al., 2016)

The findings of system simulations that have been given by (Hüsing et al., 2016) indicate that critical frost conditions and exhaustion are what prevent the area of an HGHX from being reduced. If there is less space between the HGHX pipes, solar thermal regeneration may prevent critical frost conditions and significantly reduce exhaustion at small HGHX areas. HGHX heat extraction and monthly solar yield analysis show that an HGHX is not a seasonal storage. However, due to its relatively great heat capacity, it may serve as a combined source for a heat pump and smooth out solar thermal heat production. Due to the low temperatures required, unglazed and maybe even inexpensive collectors may be utilized. As a consequence, solar thermal applications are made possible at low temperatures, with little or no impact on the possibility for summer yields to be used directly (Hüsing et al., 2016).

### **2.3 Modelization**

The modeling of a solar-assisted heat pump system involves creating a mathematical or computer-based representation of the system's behavior. To model a solar-assisted heat pump system, the relevant physical phenomena, and relationships need to be identified, quantified, and incorporated into the model. This can include the solar radiation intensity, the efficiency of the solar thermal collector, the performance of the heat pump, and the thermal properties of the building and its heating system. The model can then be used to simulate the behavior of the solar-assisted heat pump system under different operating conditions and to predict its performance, it can also be used to optimize the design of the system and to evaluate the economic and environmental benefits of different systems configurations and operating strategies. There is three common software used in simulating and incorporating the mathematical models of solar-assisted heat pump systems.

- TRNSYS

TRNSYS (Transient System Simulation Tool) is a well-known simulation software used for modeling renewable energy systems, including solar-assisted heat pumps. It offers a wide range of models for simulating different components of the system, such as heat pumps, solar collectors, and storage tanks. TRNSYS can simulate the dynamic behavior of the system and provide detailed information on energy use, energy savings, and carbon emissions.

- EnergyPlus

EnergyPlus is a building energy simulation software that can simulate the performance of solar-assisted heat pump systems. It uses a detailed building model to simulate the energy use of the building and the solar-assisted heat pump system. EnergyPlus can simulate the impact of weather conditions on the system's performance and provide detailed reports on energy use, energy savings, and carbon emissions.

- MATLAB

MATLAB is a numerical computing software that is commonly used for simulating and modeling various engineering systems, including solar-assisted heat pumps. It offers a range of modeling and simulation tools that allow engineers and researchers to develop complex models and analyze the system's performance. MATLAB can also be used to develop control algorithms and optimize the system's operation.



### 2.3.1 Mathematical modeling of a solar-assisted heat pump system

#### 2.3.1.1 Solar Thermal Collectors

Solar thermal collectors are the primary component of the solar-assisted heat pump system. They capture solar radiation and convert it into thermal energy. The most common types of solar thermal collectors used in solar-assisted heat pumps are flat plate collectors and evacuated tube collectors. Flat plate collectors consist of a flat absorber plate that absorbs solar radiation and transfers it to a fluid flowing through the collector. Evacuated tube collectors, on the other hand, consist of a series of tubes with a vacuum between them. The tubes absorb solar radiation and transfer it to a fluid flowing through them. Nuntaphan et al. (2009) modeled the solar collector with its thermal efficiency as the primary solar collector evaluation factor.

$$\eta_{th} = F_R(\tau\alpha) - F_R \frac{T_{wc,i} - T_a}{I_t} \quad (1)$$

where  $\eta_{th}$  is the thermal efficiency,  $F_R$  is the heat removal factor that is connected with the efficiency factor,  $(\tau\alpha)$  is the transmittance absorption coefficient of glazing cover,  $T_{wc,i}$  is the working liquid temperature at the inlet of the solar collector;  $T_a$  is the ambient temperature;  $I_t$  is the solar irradiation (Freeman et al., 2017). The collector system is modeled as operating under quasisteady-state conditions with steady-state equations, disregarding the collectors' thermal capacity. The collector's thermal efficiency is represented by equation (2).

$$\eta_{col} = \eta_0 - c_1 \frac{\bar{T} - T_{am}}{G} - c_2 \frac{(\bar{T} - T_{am})^2}{G} \quad (2)$$

Where  $\eta_{col}$  collector Efficiency,  $\eta_0$  the zero-loss optical efficiency,  $c_1, c_2$  Heat loss terms,  $\bar{T}$  Mean temperature in the collector,  $T_{am}$  ambient temperature,  $G$  Solar irradiance.

The solar collector can also be moderated by its outlet temperature equation, which can be demonstrated from the energy balance equation of the collector.

$$\frac{\text{accumulated energy}}{\text{time}} = \frac{\text{input energy}}{\text{time}} - \frac{\text{output energy}}{\text{time}} \quad (3)$$

$$\frac{\text{accumulated energy}}{\text{time}} = \frac{d(\rho c V_c T_{ou})}{d\tau} \quad (4)$$

Where  $\rho$  density of the heat transfer medium in the collector  $kg/m^3$ ,  $c$  specific heat of the heat transfer medium in the collector  $J/kg \text{ } ^\circ C$ ,  $V_c$  filling volume of the collector  $m^3$ ,  $T_{ou}$  the outlet temperature of the collector  $^\circ C$ ,  $\tau$  time, s.

$Q_s$  the heat energy collected by the collector absorber,

$$\frac{\text{input energy}}{\text{time}} = Q_s = I A_c a\alpha \quad (5)$$

Where  $I$  solar irradiation intensity at the collector surface  $W/s^2$ ,  $A_c$  Collector absorber surface,  $m^2$ , a light transmittance of the collector cover,  $\alpha$  radiation absorbing coefficient of the collector absorber.

$Q_l$  the heat loss of the collector to the environment

$$\frac{\text{output energy}}{\text{time}} = Q_l = UA_c (T_{abs} - T_a) \quad (6)$$

Where  $U$  collector heat loss coefficient to the environment  $W/m^2 \text{ } ^\circ C$ ,  $A_c$  collector absorber surface  $m^2$ ,  $T_{abs}$  collector absorber temperature  $^\circ C$ ,  $T_a$  ambient temperature  $^\circ C$ .

$$Q_f = \dot{m}c (T_{ou} - T_{in}) \quad (7)$$

Where  $c$  specific heat of the heat transfer medium passing through the collector,  $J/kg \text{ } ^\circ C$ ,  $T_{ou}$  collector outlet temperature  $^\circ C$ ,  $T_{in}$  inlet temperature  $^\circ C$ .

Based on the previous, the energy balance equation of the collector is :

$$\frac{d(\rho c V_c T_{ou})}{d\tau} = IA_c \alpha \alpha - UA_c (T_{abs} - T_a) + \dot{m}c T_{in} - \dot{m}c T_{ou} \quad (8)$$

When calculating the heat loss, instead of the collector absorber temperature  $T_{abs}$ , the average collector temperature  $T_{av} = \frac{T_{ou} + T_{in}}{2}$  (9)

There is a thermal resistance between the absorber and the heat transfer medium, this effect being taken into account by the heat transfer or heat transfer correction factor  $F'$ , which characterizes the efficiency of the heat transfer between the absorber surface and the heat transfer fluid.

$$\rho c V_c \frac{d T_{ou}}{d\tau} = IA_c F' \alpha \alpha - UA_c F' (T_{av} - T_a) + \dot{m}c (T_{in} - T_{ou})$$

For collector performance tests and measurements, the products  $F' \alpha \alpha$  and  $UF'$  are used.  $F' \alpha \alpha$  is also called optical efficiency and is denoted by  $\eta_0$ , while the product of  $UF'$  is called the total heat loss factor of the collector and is denoted by  $U_L$ .

$$\frac{d T_{ou}}{d\tau} = \frac{Ac \eta_0}{\rho c V_c} I - \frac{Ac U_L}{\rho c V_c} (T_{av} - T_a) + \frac{\dot{m}}{\rho V_c} (T_{in} - T_{ou}) \quad (10)$$

### 2.3.1.2 Heat Pump

The heat pump is the heart of the solar-assisted heat pump system. It is responsible for extracting heat from the solar thermal collectors and the surrounding air and transferring it into the building. The heat pump uses a refrigeration cycle to transfer heat from one location to another. During the heating mode, the heat pump extracts heat from the solar thermal collectors or the surrounding air and transfers it to the building. During the cooling mode, the heat pump extracts heat from the building and transfers it to the solar thermal collectors or the surrounding air.

### Compressor

The compressor is the most critical component of the heat pump. It compresses the refrigerant gas, increasing its temperature and pressure, and moves it through the system. The compressor requires a considerable amount of energy to operate, and its efficiency directly impacts the overall efficiency of the solar-assisted heat pump system (Nuntaphan et al., 2009). The model of the compressor is based on the pressure ratio of the compressor.

$$\frac{P_{cp,o}}{P_{cp,i}} = \left( \frac{T_{cp,o} + 273.15}{T_{cp,i} + 273.15} \right)^{\frac{n}{n-1}} \quad (11)$$

Where  $P_{cp,o}$  and  $P_{cp,i}$  is the outlet and inlet pressure of the compressor,  $T_{cp,o}$  and  $T_{cp,i}$  is the outlet and inlet temperature of the refrigerant, and  $n$  is the polytropic index.

### Condenser

The condenser is the component where the refrigerant gas releases heat and the heat pump transfers it to the building or the solar thermal collectors. The refrigerant gas is cooled in the condenser, and its state changes from a gas to a liquid (Nuntaphan et al., 2009).

$$Q_{cd} = \dot{m}_{ws} CP_{ws} (T_{wcd,o} - T_{wcd,i}) = \dot{m}_r (h_{cd,i} - h_{cd,o}) \quad (12)$$

$$\text{And} \quad Q_{cd} = Q_{ev} + W_{cp} \quad (13)$$

where  $\dot{m}_{ws}$  is the mass flow rate of water from a storage tank,  $h_{cd,i}$  and  $h_{cd,o}$  are the inlet and outlet enthalpies of refrigerant, and  $T_{wcd,i}$  and  $T_{wcd,o}$  are the inlet and outlet temperatures of water in a condenser, respectively and  $W_{cp}$  is the power of the compressor.

### Evaporator

The evaporator is the component where the refrigerant gas absorbs heat from the solar thermal collectors or the surrounding air. The refrigerant gas is heated in the evaporator, and its state changes from a liquid to a gas (Nuntaphan et al., 2009).

$$Q_{ev} = \dot{m}_w CP_w (T_{wev,i} - T_{wev,o}) = \dot{m}_r (h_{ev,o} - h_{ev,i}) \quad (14)$$

where  $Q_{ev}$  is the heat transfer rate of the evaporator,  $CP_w$  is the specific heat of water;  $\dot{m}$  is the mass flow rate of water from a solar collector, and  $h_{ev,i}$  and  $h_{ev,o}$  are the inlet and the outlet enthalpies of refrigerant,  $T_{wev,i}$  and  $T_{wev,o}$  are the inlet and the outlet temperatures of water at an evaporator, respectively.

### Expansion Valve

The expansion valve is a critical component that regulates the flow of refrigerant gas into the evaporator. It reduces the pressure and temperature of the refrigerant gas, allowing it to absorb heat from the solar thermal collectors or the surrounding air. The passage of the refrigerant through the expansion valve can be considered an isenthalpic process. Its equation can be expressed as follows (Nuntaphan et al., 2009).

$$h_{ex.i} = h_{ex.o} \quad (15)$$

where  $h_{ex.i}$  and  $h_{ex.o}$  are the enthalpy of refrigerant at the inlet and outlet of the expansion valve.

### Heat Exchanger

The heat exchanger is a component that transfers heat between the refrigerant and the heat transfer fluid. In a solar-assisted heat pump system, the heat exchanger transfers heat between the refrigerant and the fluid flowing through the solar thermal collectors.

### Storage Tank

The storage tank is a component that stores the heat transfer fluid from the solar thermal collectors. The fluid is heated by solar thermal collectors and transferred to the storage tank. The storage tank then provides a source of hot water for the building, reducing the demand for energy to heat water. The thermal energy from the evaporator is used to heat the water in the reservoir, and the temperature of the water can be determined by:

$$M_s C P_w \left( \frac{dT_s}{dt} \right) = Q_{cd} - (UA)_L (T_s - T_a) \quad (16)$$

where  $M_s$  is the mass of water in the storage tank,  $T_s$  is the temperature of water in the storage tank,  $t$  is time, and  $(UA)_L$  is the overall coefficient of heat loss from the storage tank (Nuntaphan et al., 2009).

### Control System

The control system is a component that monitors and controls the operation of the solar-assisted heat pump system. It regulates the flow of refrigerant and heat transfer fluid, ensuring optimal performance and efficiency. The control system also monitors the temperature of the storage tank, the solar thermal collectors, and the building, adjusting the operation of the heat pump to meet the heating and cooling demands of the building.

## **2.4 Conclusion**

The integration of solar thermal collectors with heat pumps can significantly increase overall energy efficiency and reduce the dependence on fossil fuels. The research conducted in this literature review has demonstrated the technical feasibility and economic viability of solar-assisted heat pumps in various applications (direct expansion solar-assisted heat pump, indirect expansion solar solar-assisted pump including the single and the double source solar-assisted heat pump). Moreover, the mathematical model of a solar-assisted heat pump system was also discussed and the different software used to simulate these models.

### 3 Materials and methods

#### 3.1 Description of the materials

This trial was carried out at the energetic building's laboratory of the Hungarian University of Agriculture and Life Sciences. The main component of the system is the heat pump which is assisted with a flat plate solar collector placed outside on the roof of the mentioned building. Moreover, the control system and the measuring instruments and sensors with data collecting software are also taking place in these experiments (Figure 18).

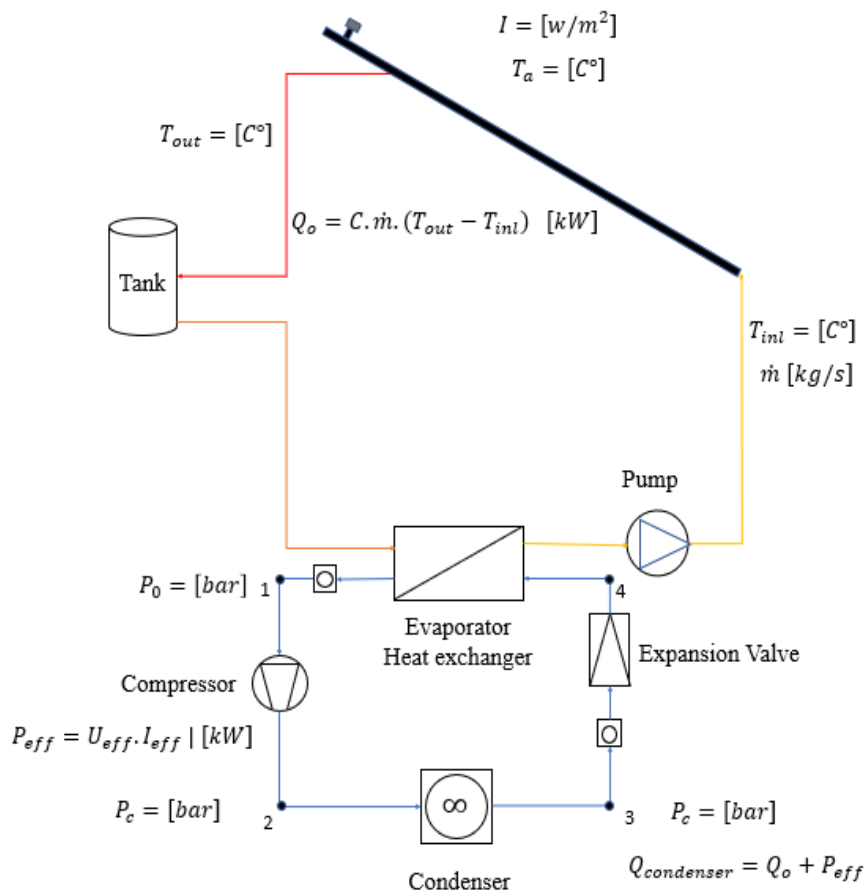


**Figure 18.** The solar-assisted heat pump system installation

##### 3.1.1 Solar collector

The solar collector used in this experiment was a flat plate collector with surface of 1.92 m<sup>2</sup>. The collector was made of copper with a black paint coating on the absorber plate to improve its thermal absorption. It was installed in a south-facing direction at an angle of 33 degrees to the horizontal, and it was mounted on a fixed frame. The solar collector was used to heat the antifreeze, which was circulated through a series of tubes inside the collector and was heated by the sunlight absorbed by the collector. The fluid temperature was measured at the inlet and outlet of the collector, and the solar irradiance and ambient temperature were also recorded during the experiment.

### 3.1.2 Heat Pump

The heat pump system is constituted of multiple components as shown in Figure 19.

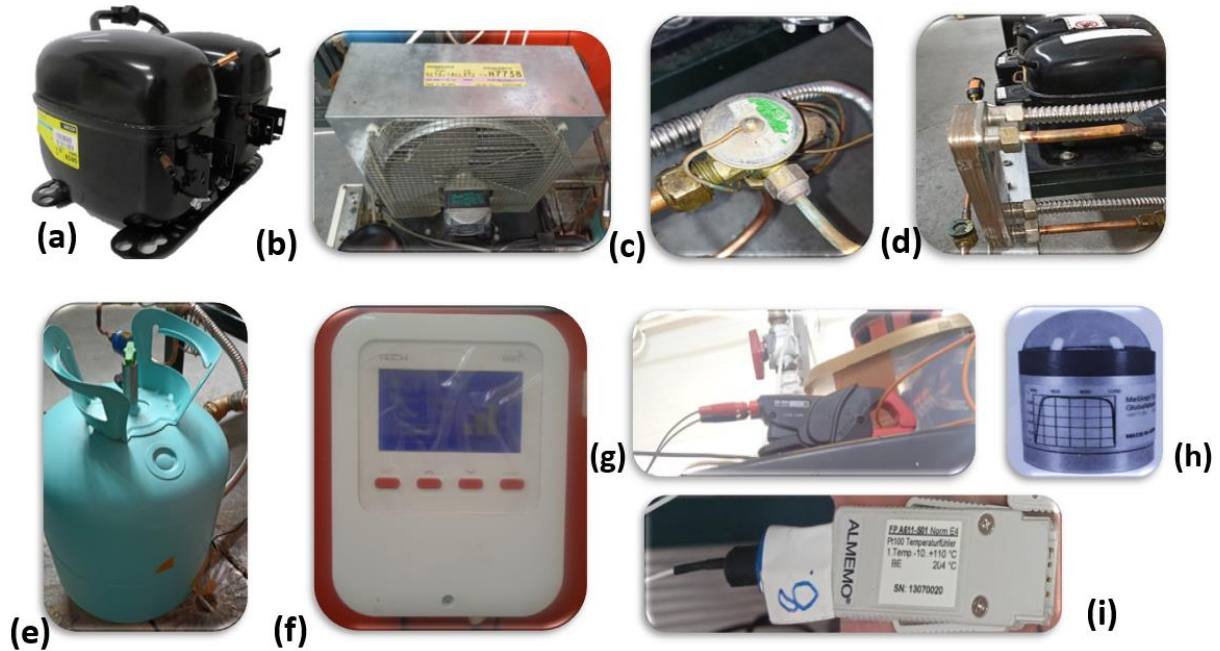


**Figure 19.** Heat pump components and measuring instruments, (a): Compressor Danfoss Twin SC18/18CL - BP - R404A R507, (b): The EBM M4Q045-DA01-55 fan, (c): The expansion valve, (d): The Heat exchanger, (e): The used tank, (f): The used thermostat, (g): The Amper clamp meter, (h): Si global radiation sensor, (i): The Pt 100 temperature sensor

#### 3.1.2.1 Compressor

The compressor used in this experiment was a Compressor Danfoss Twin SC18/18CL - BP - R404A R507 with specific characteristics set in Table.3. The compressor was designed to handle R407c refrigerant. The compressor was integrated into the heat pump assembly and was located beside the evaporator and in front of the condenser. The refrigerant inlet temperature and outlet temperature were measured, as well as the compressor power consumption was measured by measuring the instantly consumed current during the experiment (Figure 19. a).

**Table 3.** The characteristics of the Compressor Danfoss Twin

|                   |                             |
|-------------------|-----------------------------|
| Displacement      | 2x17,69                     |
| Fluid             | R404a, r448a , r449a, r452a |
| Application range | -45/-5                      |
| Application       | LBP/MBP                     |
| I.max (a)         | 2x10,58                     |
| Tension (v)       | 240/1/50                    |
| Startup           | CSR                         |
| Ø suction         | 16                          |
| Ø delivery        | 6,2                         |
| Dimensions (mm)   | 326x320x259                 |

### *3.1.2.2 Condenser*

The condenser used in this study was an axial fan as shown in Figure 19. b that was operated at a speed of 1300 revolutions per minute (RPM). The fan had a length of 40cm, width of 32 cm and the height of 10 cm, with 4 rows of tubes. The airflow rate of the fan is up to 160 cubic meters per hour, it is rated for operation at 230 volts AC and the maximum power consumption by the fan is always around 14 watts. The temperature range at which the fan was expected to operate was between 30 and 60 degrees.

### *3.1.2.3 Expansion valve*

The expansion valve used in this study is a mechanical valve designed for use with refrigerant R404a, R22, R407c. The valve has maximum refrigeration power of 3kW, and creates a pressure drop of approximately 8 bar in these experiments. The expansion valve is installed downstream of the condenser and upstream of the evaporator in the heat pump system (Figure 19.c).

### *3.1.2.4 Heat exchanger-Evaporator*

For this study, a CBH 16-9H SWEP-sized plate heat exchanger with a heat transfer capacity of 35 kW was used. The heat exchanger featured compact, brazed plate construction made of high-quality stainless-steel plates, ensuring both durability and resistance to corrosion. The overall heat transfer coefficient of the CBH 16-9H heat exchanger was 4500 W/m<sup>2</sup>K in this experiment. The CBH 16-9H was mounted horizontally in the experimental setup (Figure 19. d).

### *3.1.2.5 Storage tank*

A vertical cylindrical tank made of stainless steel with a capacity of 100 liters was used in the experimental setup. The tank was insulated with 2 inches of closed-cell foam insulation to reduce heat loss to the environment. The tank was equipped with an electric heater with a rated power of 3 kW to maintain the temperature of the water stored in the tank. The water inlet and outlet pipes were connected to the tank using stainless steel fittings with a diameter of 1 inch. The water level in the tank was monitored using a level sensor, and the temperature of the water was measured using a thermocouple inserted through a small opening in the tank wall. The tank was operated at a constant temperature of 50°C throughout the experimental period (Figure 19. e).

### *3.1.2.6 Control system*

To control the inlet temperature of the solar collector, a digital thermostat was used. The thermostat was connected between the storage tank and the solar collector (Figure 19. f).

## *3.1.3 Data collection material*

For later utilization of measured data, it was necessary to use a recording system where we can read and record different instantly measured temperatures and solar irradiation as well as the consumed current by the compressor.

### 3.1.3.1 ALMEMO system

To record experimental data, an ALMEMO system was used as shown in Figure 19. The system consisted of a data acquisition device and software for collecting, processing and storing experimental data. The data acquisition device was connected to various sensors throughout the experimental setup, including thermocouples, pressure sensors, and flow meters. The software was used to configure the data acquisition device and set up data logging parameters. The system was configured to record data at a rate of one sample per second, and the data was stored on a computer for later analysis.

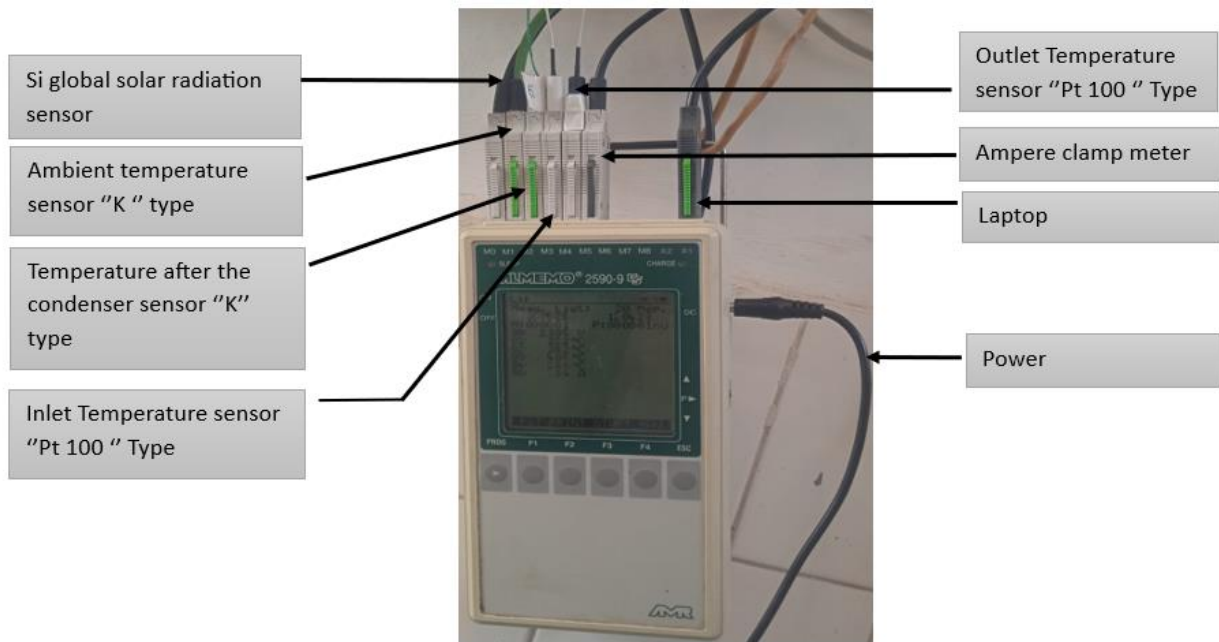


Figure 20. ALMEMO system

### 3.1.3.2 The solar irradiation instruments

The used sensor is shown in Figure 19. It was a Si global radiation sensor that measures the global radiation, based on a silicon diode with a diffusor and PMMA-dome. Especially suitable as a reference for photovoltaic systems, including built-in measuring amplifiers. The measuring results are allowing conclusions about medical and bio-logical connections compared to other spectral ranges. The measuring head can be used in medical and biological research, weather information and forecast systems, climate research, agriculture, and public information in general. More information can be found in Appendix 1.

### 3.1.3.3 The temperature sensors instruments

The measurement of temperature in this work is a necessary and critical task, and the measuring instruments should be highly accurate, during these experiments "Pt 100" -Type and "K"- type are the used sensors.

#### "Pt 100"-Type

To monitor the temperature during the experiments, a Pt100 temperature sensor (model number 13070020, Manufacturer by ALMEMO FP A611-S01 Norm E4) was used. The sensor was



factory-calibrated prior to use and had an operating range of -10 to 110 °C. The accuracy of the sensor was  $\pm 0.1$  °C, and the resolution was 0.01 °C. The sensor was mounted at a THE inlet and the outlet of the solar collector to ensure consistent temperature measurements. To ensure the accuracy of the temperature measurements, the Pt100 temperature sensor was connected to the ALMEMO system, which recorded the temperature readings at regular intervals throughout the experiment (Figure 19 i).

#### “K”-Type

Another temperature sensor used in the experiment was the K-type thermocouple K-type thermocouples, these sensors are widely used in various industrial and scientific applications due to their versatility, ruggedness, and high-temperature measurement capability. The sensor was calibrated using a reference thermometer before the experiment to ensure accurate readings. The K-type thermocouple had an operating range of -10 to +110 °C and a rated accuracy of  $\pm 0.1$  °C, whichever was greater. The thermocouple was inserted into the system between the condenser and the expansion valve to measure the after-condenser temperature. The temperature readings from the K-type thermocouple were recorded using ALMEMO system, which recorded the temperature readings at regular intervals throughout the experiment.

#### *3.1.3.4 Amper clamp meter*

An amper clamp meter (FE A604-9 Teller R1E4, Manufacturer by ALMEMO) was used to measure the current in the circuit during the experiment. The amper clamp meter had a range of 1 to 150 A and a resolution of 0.01 amperes. During the experiment, the amper clamp meter was connected to the power cable of the compressor in order to measure the consumed current in the compressor per second. The data obtained from the amper clamp meter was recorded in ALMEMO system (Figure 19. g).

### **3.2 Description of the methods**

#### *3.2.1 The schema of the executed solar-assisted heat pump system*

The executed solar-assisted heat pump system as shown in Figure 19 is constituted of two main circuits the antifreeze circuit and the refrigerant circuit; in this study, I am going to focus on the antifreeze circuit, as the aim of the study is to investigate the resultant outlet temperature under same solar irradiation over different days taking into account that the mass flow of the Antifreeze (the heat transfer medium circulate inside the solar collector) is constant, and the inlet temperature is the controlled variable, The experiments take place during three days in each day, we set different inlet temperature of the solar collector and we see how the outlet temperature is changing in almost same values of external condition in each day. We also verify the hypothesis says the lowest inlet temperature of the solar collector the highest system performance will be. In the experiments we also investigate the change of the extracted heat according to the inlet temperature and the external conditions during the day, then the coefficient of performance of the whole system including the heat pump.

### 3.2.2 The use of the ALMEMO system

To maintain a constant inlet temperature of the solar collector, a digital thermostat was used to control the inlet temperature during the day around an average of 10°C in the first day 7°C in the second day and 7°C in the last day. The thermostat was equipped with a temperature sensor type NTC that was installed at the inlet of the solar collector. Another temperature sensor type PT 100 was installed at the outlet of the solar collector to monitor the temperature of the antifreeze in order to investigate the change of the outlet temperature as well as the calculation of the extracted heat and both of the temperature sensors were connected to the ALMEMO system in order to instantly record the collected data. The ambient temperature and solar irradiation were also measured during the experiments and record in the ALMEMO system in same time as the solar collector temperatures. The instantly consumed current in the compressor was also measured by using an Amper clamp meter in order to calculate the COP of the whole system. The refrigerant circuit in the system is strongly depend on the inlet temperature when the inlet temperature drops below the fixed value the Heat pump shuts off, the start of the next heat pump cycle will be when the inlet temperature reaches again the previously set temperature point.

## 3.3 Simulation

### 3.3.1 MATLAB software

MATLAB Simulink software was used to model and simulate the outlet temperature of the solar collector change under the measured external condition and the measured inlet temperature of the solar collector. The model was parameterized and simulated using default settings. The model was verified and validated against experimental data, and the limitations associated with using Simulink were addressed by performing sensitivity analyses and uncertainty quantification.

#### 3.3.1.1 The chosen mathematical model

The chosen mathematical model for the outlet temperature as a function of time is the following

$$\frac{dT_{ou}(\tau)}{d\tau} = \frac{A_c \eta_0}{c} I(\tau) - \frac{A_c U_L}{c} (T_{av}(\tau) - T_a(\tau)) + \frac{\dot{v}_c}{V_c} (T_{in}(\tau) - T_{ou}(\tau)) \quad (17)$$

Where the origin of the formula comes from the energy balance equation of the flat-plate collector;

$$\rho c V_c \frac{dT_{ou}(\tau)}{d\tau} = A_c \eta_0 I(\tau) - U_L A_c (T_{av}(\tau) - T_a(\tau)) + \dot{m}c(T_{in}(\tau) - T_{ou}(\tau)) \quad (18)$$

$\rho c V_c \frac{dT_{ou}(\tau)}{d\tau}$  represent the rate of change in the amount of heat accumulated by the heat transfer medium in the collector,  $A_c \eta_0 I(\tau)$  is the heat energy collected by the collector absorber,  $U_L A_c (T_{av}(\tau) - T_a(\tau))$  represent heat loss of the collector to the environment, where  $\dot{m}c(T_{in}(\tau) - T_{ou}(\tau))$  is the heat transferred by the heat transfer medium passing through the collector or the usable heat ( Figure 21).

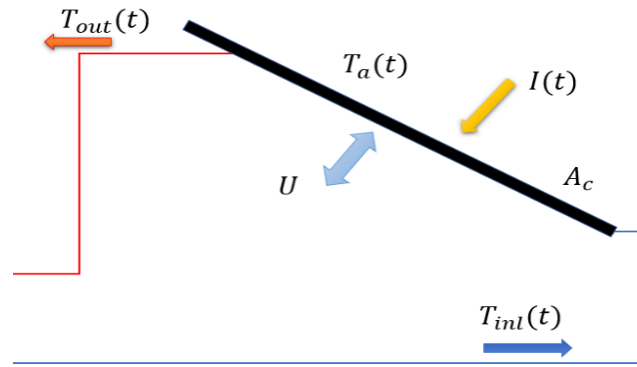


**Figure 21.** Sketch of a flat-plate collector

Where :

$C = \rho c V_c$  : heat capacity of antifreeze,  $\text{JK}^{-1}$ .

$\rho$  : density of the antifreeze  $\text{kg m}^{-3}$ .

$c$  : specific heat of the antifreeze  $\text{J kg}^{-1} \text{K}^{-1}$ .

$V_c$  : filling volume of the collector  $\text{m}^3$ .

$A_c$  : Collector absorber surface  $\text{m}^2$ .

$\eta_0$  : optical efficiency of the collector.

$I$  : solar radiation intensity at the collector surface

$\text{Wm}^{-2}$ .

$U_L$  : total heat loss factor of the collector  $\text{W m}^{-2} \text{K}^{-1}$ .

$T_a$  : ambient temperature  $^{\circ}\text{C}$ .

$T_{in}$  : Collector inlet Temperature  $^{\circ}\text{C}$ .

$T_{ou}$  : Collector outlet temperature  $^{\circ}\text{C}$ .

$T_{av}$  : average collector temperature  $^{\circ}\text{C}$ .

$\dot{v}_c$  : volumetric flow of the antifreeze passing through a collector  $\text{m}^3 \text{s}^{-1}$ .

$\tau$  : time s.

- The optical efficiency of the collector  $\eta_0$  and the total heat loss coefficient  $U_L$

**Table 4.** Typical values of optical efficiency  $\eta_0$  and total heat loss factor  $U_L$  for different types of collectors

| Collector type                                  | Temperature range, $^{\circ}\text{C}$ | $\eta_0$ | $U_L \text{ W m}^{-2} \text{C}^{-1}$ |
|---|---------------------------------------|----------|--------------------------------------|
| Without cover                                   | 10-40                                 | 0.90     | 15-25                                |
| With single-layer glazing                       | 10-60                                 | 0.80     | 7                                    |
| Double glazing                                  | 10-80                                 | 0.65     | 5                                    |
| Single-layer glazing, selective coated absorber | 10-80                                 | 0.80     | 5                                    |
| Vacuum tube                                     | 10-130                                | 0.70     | 2                                    |

Grouping the input and the output variables of the collector model according to control aspects

- State variables:  $T_{ou}(\tau)$
- Controlled variables:  $T_{ou}(\tau)$
- Input variables:
  - Manipulated variables:  $\dot{v}_c$
  - Disturbances:  $I(t), T_a(t), T_{in}(t)$
- Parameters:  $A_c, \rho, c, V_c, U_L$

The executed model in MATLAB SIMULANK is shown in Figure 22.

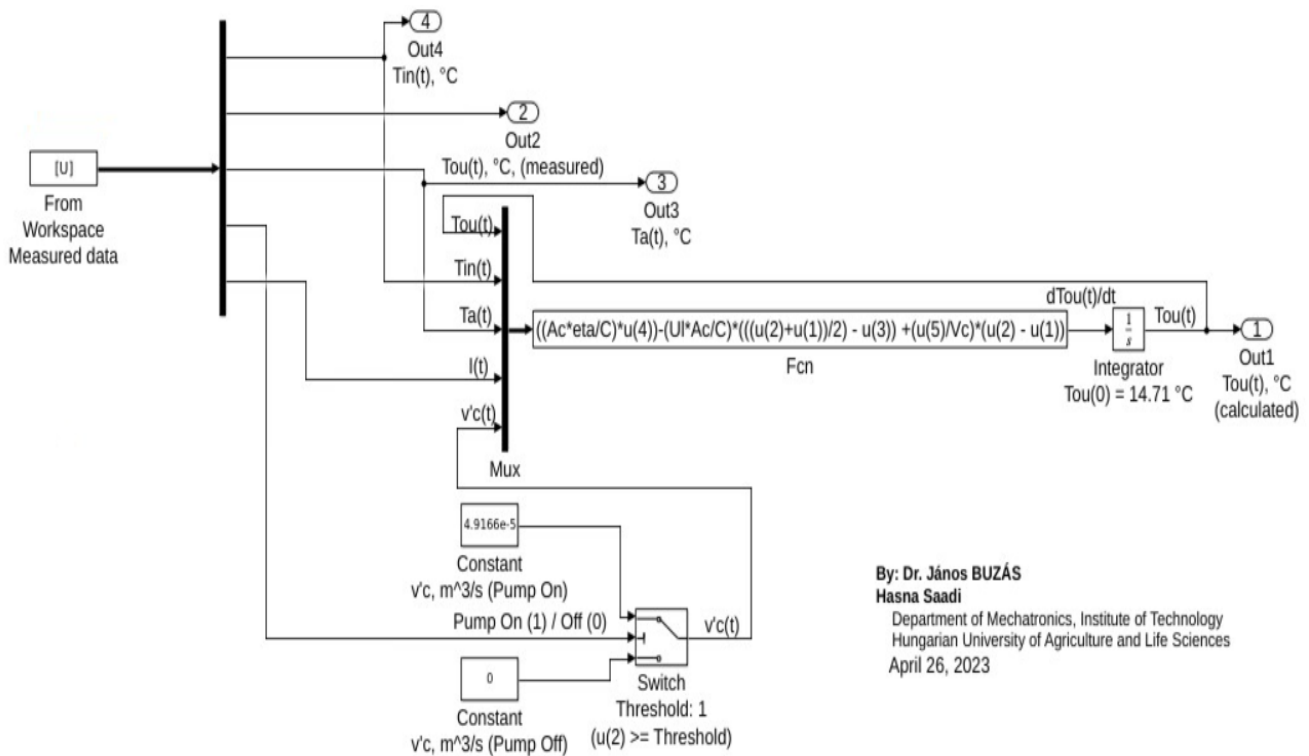


Figure 22. The solar collector model in MATLAB

## 4 Results and Discussion

In the present investigation, experiments with a flat plate solar collector were conducted on three days. These day's distributions of ambient temperature and incident solar irradiation are depicted in Figure 23, Figure 24 and Figure 25. The data in Figure 23 indicate that the ambient temperature and solar irradiation were varied from 11 to 24 degrees Celsius and 500 to 1100 watts per square meter, respectively, with an average of 873 W/m<sup>2</sup> in solar irradiation and an average of 18.24°C concerning the ambient Temperature.

### 4.1 The measured External Conditions

1<sup>st</sup> Day measurements

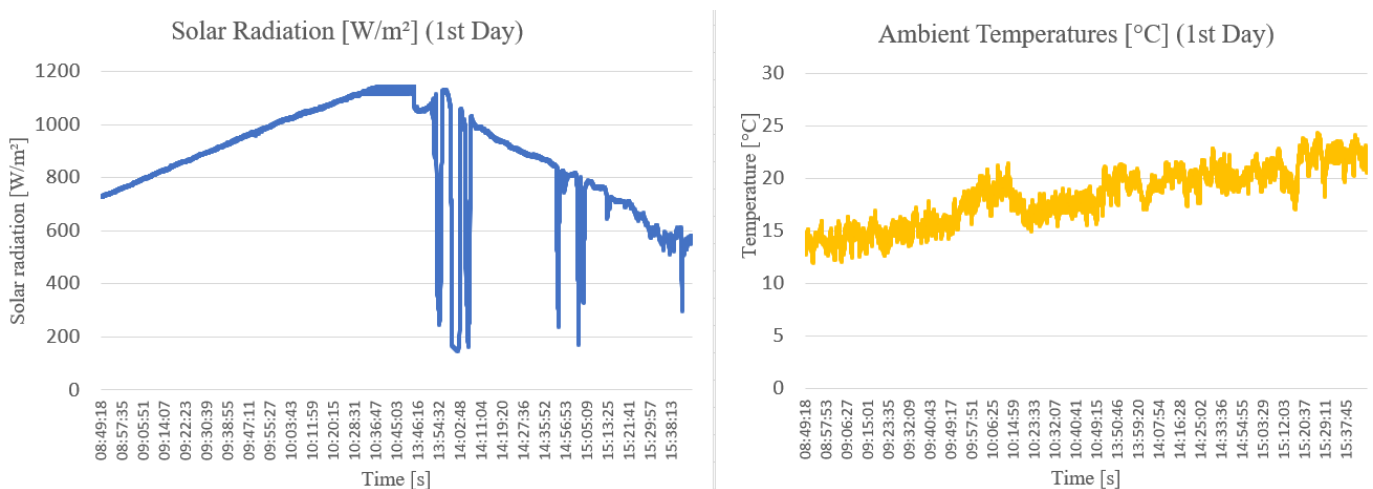


Figure 23. The solar irradiation and ambient temperature during the 1<sup>st</sup> day of experiment

**Table 5.** The average value of the solar irradiation and ambient temperature during the first day

| Solar irradiation [W/m <sup>2</sup> ] | Ambient Temperature [°C] |
|---------------------------------------|--------------------------|
| 873.49                                | 18.27                    |

- 2<sup>nd</sup> Day measurements

The data in Figure 24 indicate that the ambient temperature and solar irradiation were varied from 10 to 29 degrees Celsius and 500 to 1100 watts per square meter, respectively during the second day, with an average of 608 W/m<sup>2</sup> in solar irradiation and an average of 19.89°C concerning the ambient Temperature.

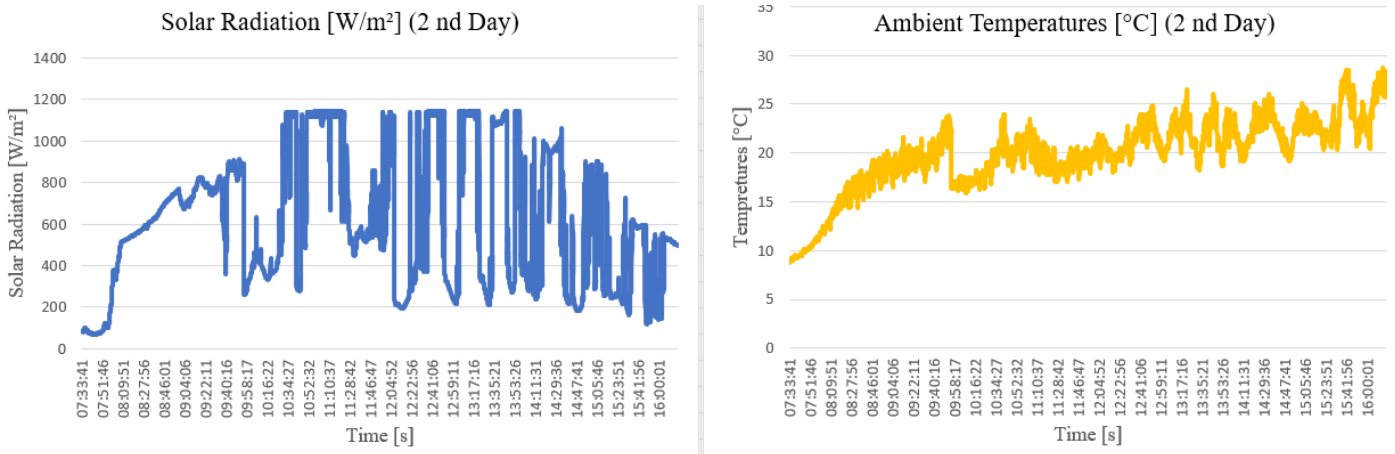


**Figure 24.** The solar irradiation and ambient temperature during the 2<sup>nd</sup> day of experiments

**Table 6.** The average value of the solar irradiation and ambient temperature during the second day

| Solar irradiation [W/m <sup>2</sup> ] | Ambient Temperature [°C] |
|---------------------------------------|--------------------------|
| 608.35                                | 19.89                    |

- 3<sup>rd</sup> Day measurements

The data in Figure 25 indicate that the ambient temperature was varied from 15 to 21 degrees Celsius and due to the cloudy nature of the day the solar irradiation can shut down to 300W/m<sup>2</sup>, as it can also reach 1150W/m<sup>2</sup> for the majority of the day, with an average of 921 W/m<sup>2</sup> and an average of 16.69°C concerning the ambient temperature.

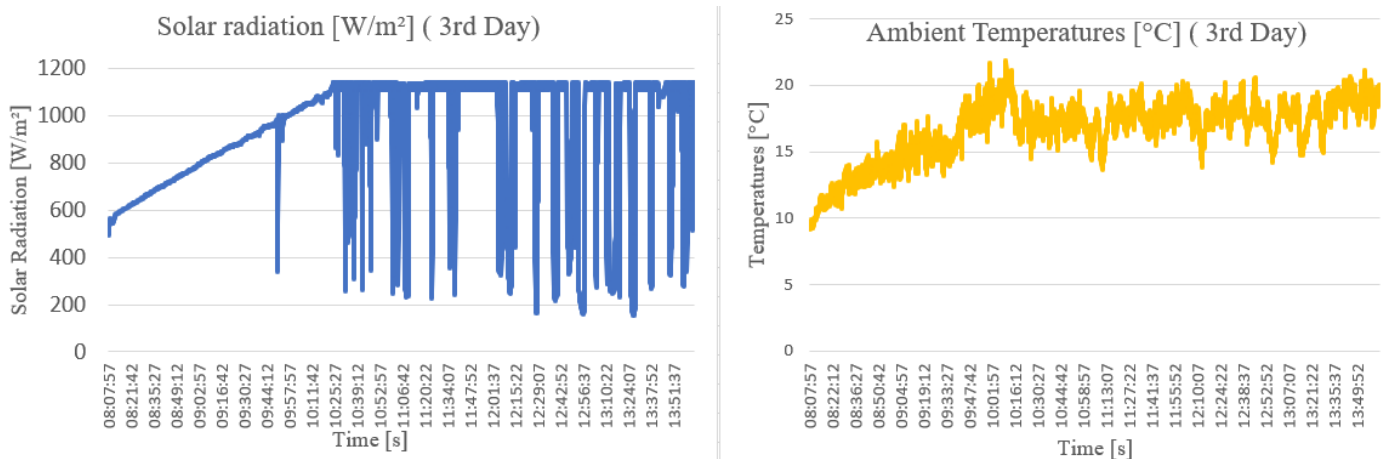


**Figure 25.** The solar irradiation and ambient temperature during the 3<sup>rd</sup> day of experiments

**Table 7.** The average value of the solar irradiation and ambient temperature during the second day

| Solar irradiation [W/m <sup>2</sup> ] | Ambient Temperature [°C] |
|---------------------------------------|--------------------------|
| 921.07                                | 16.691                   |

## 4.2 The measured outlet temperature of the solar collector

The change of the outlet temperature is investigated based on observing the impact of inlet temperature, if we consider the flow rate of the heat transfer medium (antifreeze) is constant during this experiment  $\dot{m} = 0.0545 \text{ kg/s}$ , and for same solar irradiation ranges (780-910W/m<sup>2</sup>), (780-910W/m<sup>2</sup>), (910-1040W/m<sup>2</sup>) and (1040-1170W/m<sup>2</sup>) in each of the three days we follow the resultant outlet temperature.

### 4.2.1 The outlet temperature under (780-910W/m<sup>2</sup>) of solar irradiation

The change of the outlet temperature of the solar collector in function of inlet temperature and ambient temperature where the solar irradiation is varying between (780-910W/m<sup>2</sup>) is presented in Figure 26, Figure 27 and Figure 28 for first, second- and third-day measurements respectively. By comparing the three days, the results from Figure 26 and Figure 27 shows that for approximately same average ambient temperature (13.9 °C, first day) and (13.38°C, third day) and same low solar irradiation range (780-910W/m<sup>2</sup>) The outlet temperature reach (18.20°C) when the average inlet temperature of the solar collector is slightly higher during the first day (12.59°C), where it only increase with 5°C (outlet temperature 12.91) where the average inlet temperature was only 7.12°C during the third day. By comparing the second- and third-day measurements Figure 27 and Figure 28 we can notice that for same irradiation range and approximately same inlet temperature of the solar collector the obtained outlet temperature was approximately the same for the second and the third day (12.53°C) and (12.91°C) respectively, without being affected by the ambient temperature that was around an average of 18.30°C in the second day and 13.38°C in the third day.

- 1<sup>st</sup> Day measurements

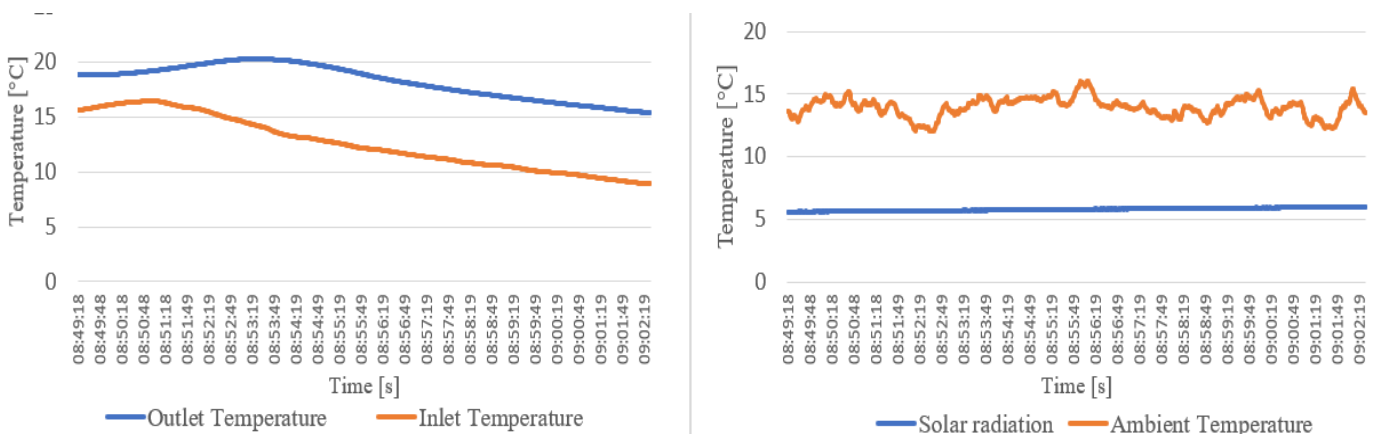


**Figure 26.** The outlet, inlet and ambient temperature in function of time under (780-910W/m<sup>2</sup>) (1st Day)

**Table 8.** The average of the ambient, inlet and the outlet temperature (780-910W/m<sup>2</sup>) (1st Day)

| Avg. Solar irradiation [W/m <sup>2</sup> ] | Ambient Temperature [°C] | Inlet Temp [°C] | Outlet Temp [°C] |
|--|--------------------------|-----------------|------------------|
| 751.4                                      | 13.93                    | 12.59           | 18.21            |

• 2nd Day measurements

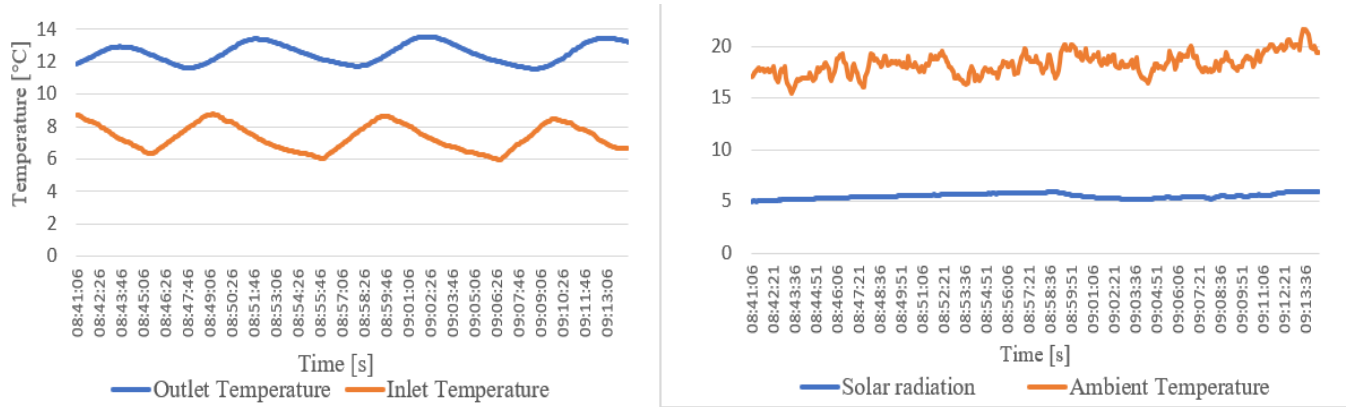


**Figure 27.** The outlet, inlet and ambient temperature in function of time under (780-910W/m<sup>2</sup>) (2<sup>nd</sup> Day)

**Table 9.** The average of the ambient, inlet and the outlet temperature (780-910W/m<sup>2</sup>) (2<sup>nd</sup> Day)

| Avg. Solar irradiation [W/m <sup>2</sup> ] | Ambient Temperature [°C] | Inlet Temp [°C] | Outlet Temp [°C] |
|--|--------------------------|-----------------|------------------|
| 715  | 18.30                    | 7.34            | 12.53            |

• 3<sup>rd</sup> Day measurements

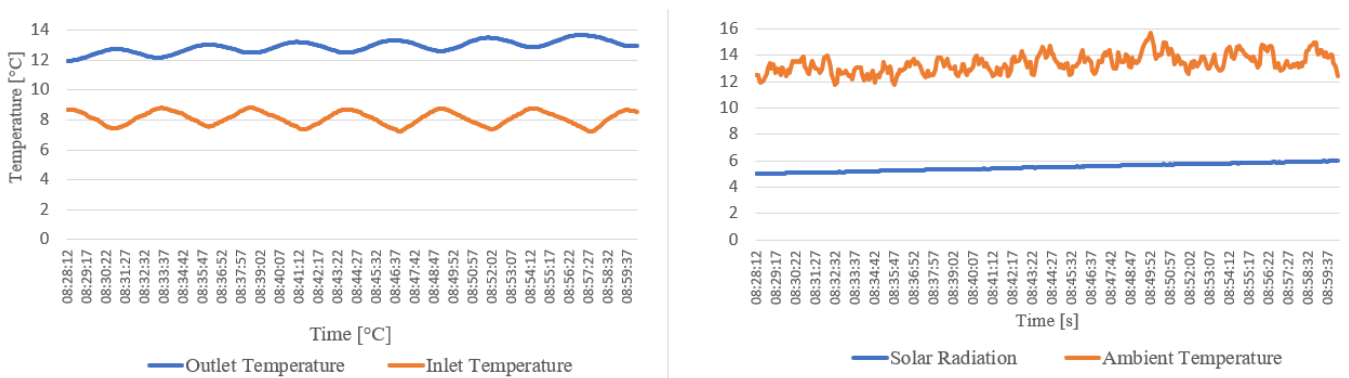


**Figure 28.** The outlet, inlet and ambient temperature in function of time under (780-910W/m<sup>2</sup>) (3<sup>rd</sup> Day)

**Table 10.** The average of the ambient, inlet and the outlet temperature (780-910W/m<sup>2</sup>) (3<sup>rd</sup> Day)

| Avg. Solar irradiation [W/m <sup>2</sup> ] | Ambient Temperature [°C] | Inlet Temp [°C] | Outlet Temp [°C] |
|--|--------------------------|-----------------|------------------|
| 716.3                                      | 13.38                    | 7.12            | 12.91            |

#### 4.2.2 The outlet temperature under (780-910W/m<sup>2</sup>) of solar irradiation

For the (780-910W/m<sup>2</sup>) range of solar irradiation the variation of outlet temperature of the solar collector is presented in Figure 29, Figure 30 and Figure 31 for first, second- and third-day measurements respectively. By comparing the three days, the results from Figure 30 and Figure 32 shows that for approximately same average ambient temperature (14.53°C, first day) and (15.07°C, third day) and same solar irradiation range (780-910W/m<sup>2</sup>) the average outlet temperature in the third day increased by 6°C from 7.69°C in the inlet temperature to 13.68°C in the outlet, where it only increase with 4°C in the first day where the average inlet temperature was 10.07°C and reach only 14.85°C. By comparing the second- and third-day measurements Figure 30 and Figure 31 we can notice that for same irradiation range (780-910W/m<sup>2</sup>) and approximately same inlet temperature of the solar collector 7.12°C (2<sup>nd</sup> day) and 7.69 (3<sup>rd</sup> day) there was a slight and neglected increase of the obtained outlet temperature in the third day with 13.68°C and 12.8°C in the second day, without really being affected by the ambient temperature that was around an average of 19.06°C in the second day and 15.07°C in the third day.

- 1<sup>st</sup> Day measurements

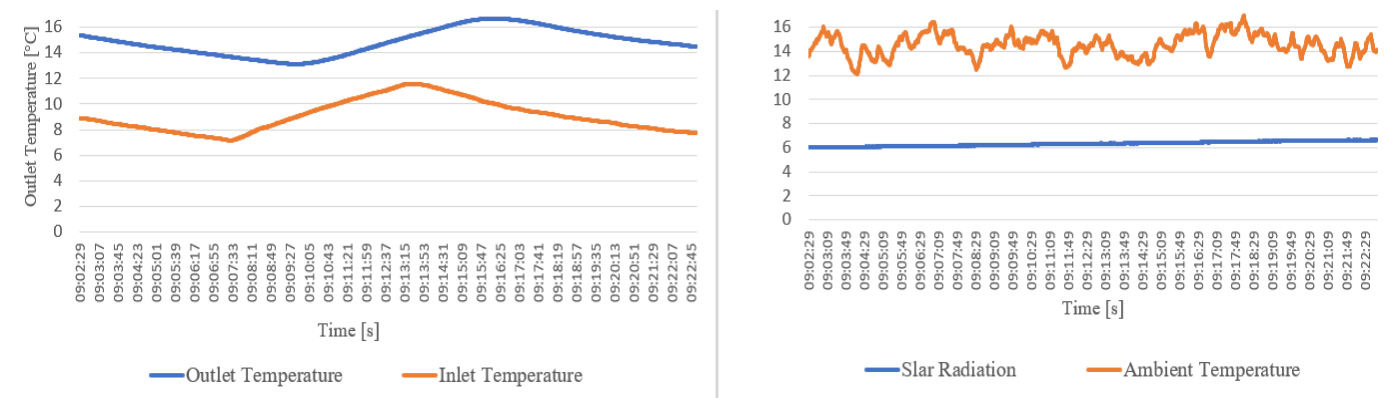


**Figure 29.** The outlet, inlet and ambient temperature in function of time under (780-910W/m<sup>2</sup>) (1st Day)

**Table 11.** The average of the ambient, inlet and the outlet temperature (780-910W/m<sup>2</sup>) (1st Day)

| Avg. Solar irradiation [W/m <sup>2</sup> ] | Ambient Temperature [°C] | inlet Temp [°C] | outlet Temp [°C] |
|--|--------------------------|-----------------|------------------|
| 821.6                                      | 14.53                    | 10.07           | 14.85            |

- 2nd Day measurements

**Table 12.** The average of the ambient, inlet and the outlet temperature (780-910W/m<sup>2</sup>) (2<sup>nd</sup> Day)

| Avg. Solar irradiation [W/m <sup>2</sup> ] | Ambient Temperature [°C] | inlet Temp [°C] | outlet Temp [°C] |
|--|--------------------------|-----------------|------------------|
| 799.5                                      | 19.06                    | 7.12            | 12.81            |



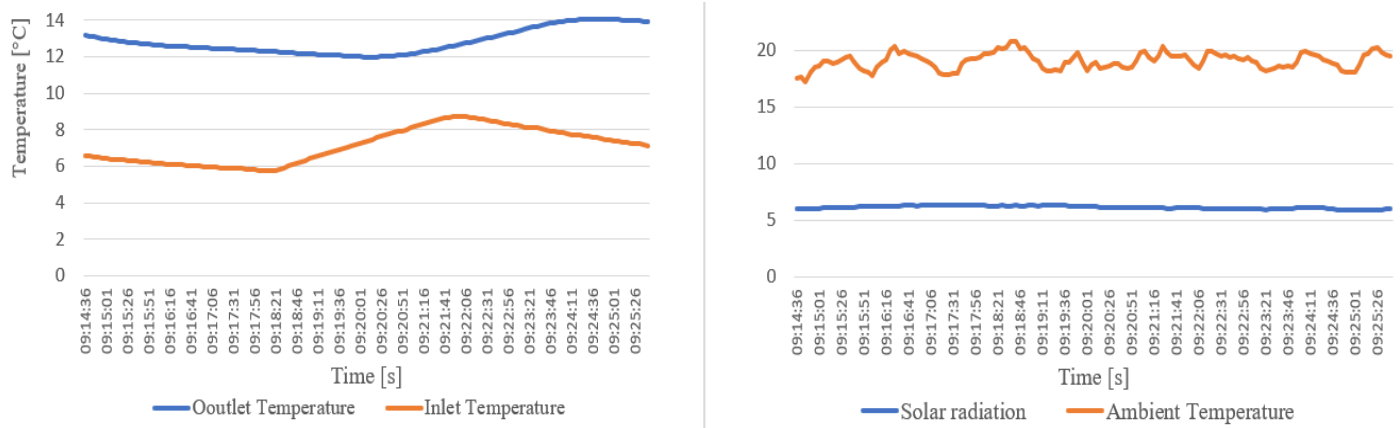


**Figure 30.** The outlet, inlet and ambient temperature in function of time under (780-910W/m<sup>2</sup>) (2<sup>nd</sup> Day)

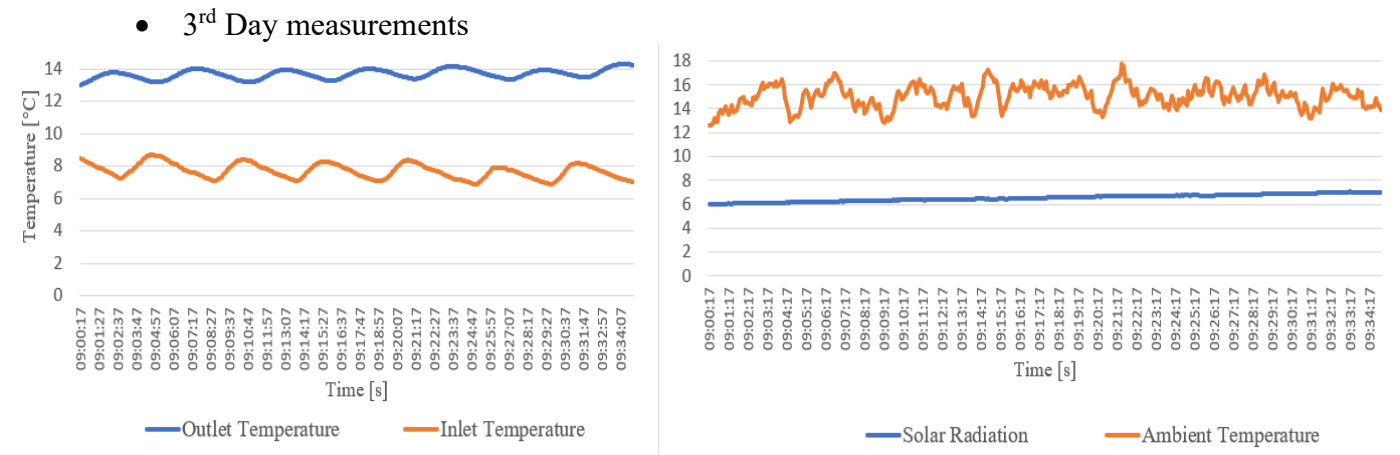


**Figure 31.** The outlet, inlet and ambient temperature in function of time under (780-910W/m<sup>2</sup>) (3<sup>rd</sup> Day)

**Table 13.** The average of the ambient, inlet and the outlet temperature (780-910W/m<sup>2</sup>) (3<sup>rd</sup> Day)

| Avg. Solar irradiation [W/m <sup>2</sup> ] | Ambient Temperature [°C] | Inlet Temp [°C] | Outlet Temp [°C] |
|--|--------------------------|-----------------|------------------|
| 848.9                                      | 15.07                    | 7.69            | 13.68            |

#### 4.2.3 The outlet temperature under (910-1040W/m<sup>2</sup>) of solar irradiation

For the (910-1040W/m<sup>2</sup>) range of solar irradiation the variation of outlet temperature of the solar collector is presented in Figure 32, Figure 33 and Figure 34 for first, second- and third-day measurements respectively. By comparing the three days, the results from Figure 33 and Figure 34 demonstrate that the outlet temperature of the solar collector change independently of the ambient temperature, where for approximately same average of the inlet temperature of the solar collector 7.18°C and 7.35°C for the second and the third day respectively, the outlet temperature is approximately the same 14.13°C (2<sup>nd</sup> day) and 14.0°C (3<sup>rd</sup> day), although the significant difference that between the average ambient temperature in the second day (23°C) and the third day (17.83°C). The results from the Figure 32 shows the same as those in Figure 31, in high solar irradiation ranges (910-1040W/m<sup>2</sup>) the temperature rises is more

significant in the outlet of the solar collector in case of lowest inlet temperatures, where in the first day measurements the temperature has risen from 5.75°C to 12.43°C with 7°C, same as the second and the third day considering the inlet temperature of the solar collector is approximately low in all the three days in this case 5.75°C, 7.18°C and 7.35°C respectively.

• 1<sup>st</sup> Day measurements

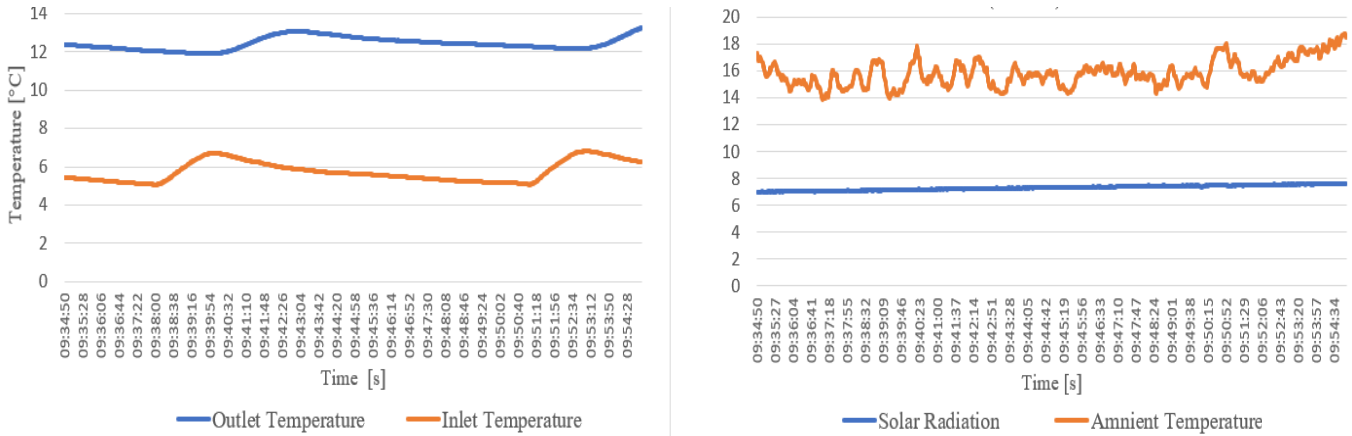


**Figure 32.** The outlet, inlet and ambient temperature in function of time under (910-1040W/m<sup>2</sup>) (1<sup>st</sup> Day)

**Table 14.** The average of the ambient, inlet and the outlet temperature (910-1040W/m<sup>2</sup>) (1<sup>st</sup> Day)

| Avg. Solar irradiation [W/m <sup>2</sup> ] | Ambient Temperature [°C] | Inlet Temp [°C] | Outlet Temp [°C] |
|--|--------------------------|-----------------|------------------|
| 950.3                                      | 15.86                    | 5.75            | 12.43            |

• 2<sup>nd</sup> Day measurements

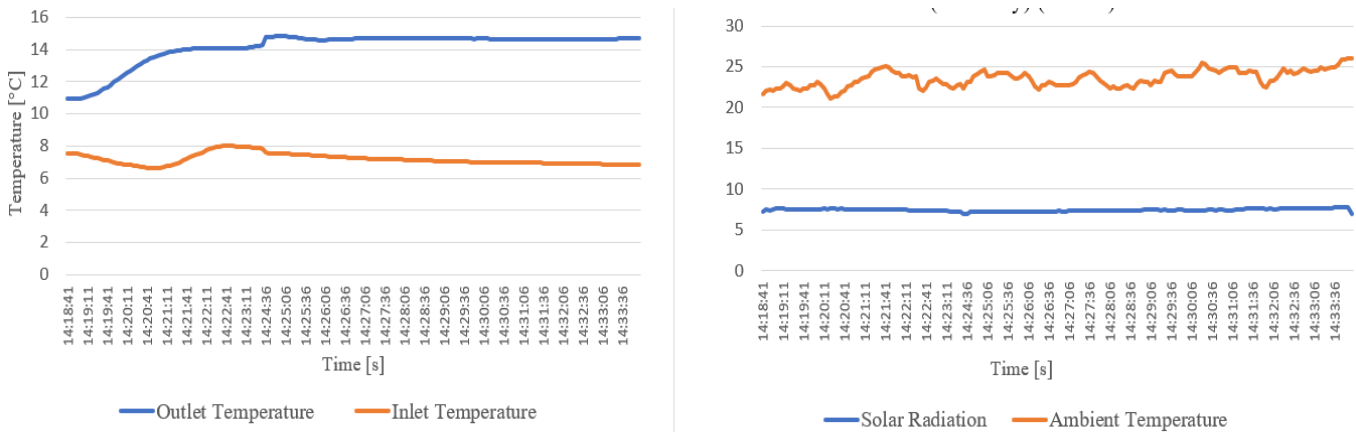


**Figure 33.** The outlet, inlet and ambient temperature in function of time under (910-1040W/m<sup>2</sup>) (2<sup>nd</sup> Day)

**Table 15.** The average of the ambient, inlet and the outlet temperature (910-1040W/m<sup>2</sup>) (2<sup>nd</sup> Day)

| Avg. Solar irradiation [W/m <sup>2</sup> ] | Ambient Temperature [°C] | Inlet Temp [°C] | Outlet Temp [°C] |
|--|--------------------------|-----------------|------------------|
| 967.2                                      | 23.56                    | 7.18            | 14.13            |

- 3<sup>rd</sup> Day measurements

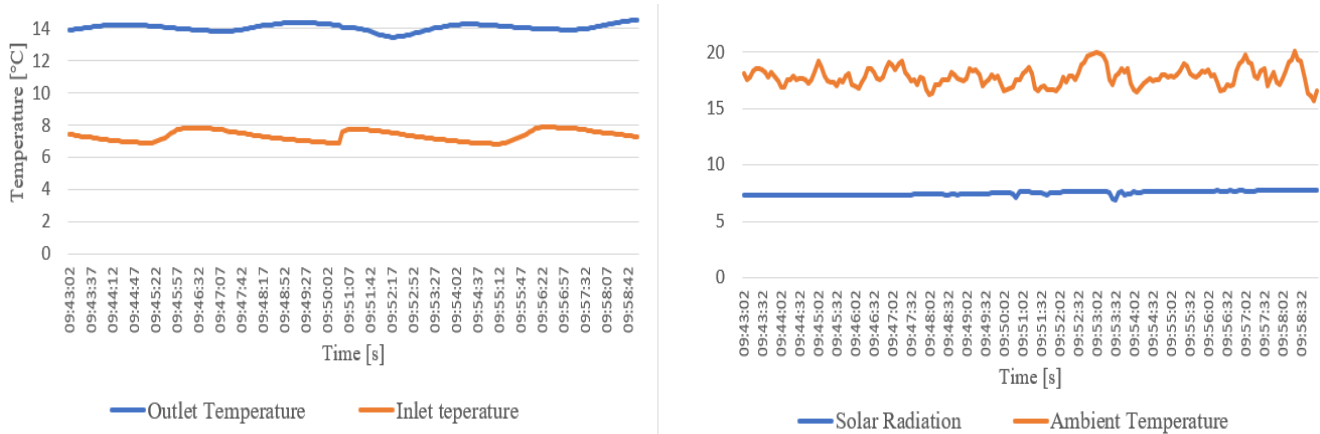


**Figure 34.** The outlet, inlet and ambient temperature in function of time under (910-1040W/m<sup>2</sup>) (3<sup>rd</sup> Day)

**Table 16.** The average of the ambient, inlet and the outlet temperature (910-1040W/m<sup>2</sup>) (3<sup>rd</sup> Day)

| Avg. Solar irradiation [W/m <sup>2</sup> ] | Ambient Temperature [°C] | Inlet Temp [°C] | Outlet Temp [°C] |
|--|--------------------------|-----------------|------------------|
| 975  | 17.83                    | 7.35            | 14.06            |

#### 4.2.4 The outlet temperature under (1040-1170W/m<sup>2</sup>) of solar irradiation

Figure 35, Figure 36 and Figure 37 show the result of the first, second- and third-day experiments respectively, for an irradiation range of (1040-1170W/m<sup>2</sup>). The results from Figure 35 and Figure 37 shows that for approximately same average ambient temperature (17.30°C, 1<sup>st</sup> day) and (17.87°C, 3<sup>rd</sup> day) and same solar irradiation range (1040-1170W/m<sup>2</sup>) the average outlet temperature in the third day increased by 8°C from 7.57°C to 15.21°C, where it only increases with 7°C in the first day where the average inlet temperature was 10.02°C and reach only 17.35°C means that the ability of the antifreeze for its outlet temperature to be increased significantly is more high when its inlet temperature is low. By comparing the second- and third-day measurements Figure 36 and Figure 37 we can notice that for same irradiation range (1040-1170W/m<sup>2</sup>) and approximately same inlet temperature of the solar collector 7.31°C (2<sup>nd</sup> day) and 7.57 (3<sup>rd</sup> day) the obtained outlet temperature was absolutely independent of the ambient temperature where the outlet temperature for the second day (Figure 36) reach 14.82°C and in the third day the outlet temperature was 15.21°C with a very slight difference of +0.13°C and without really being affected by the ambient temperature that was around an average of 22°C in the second day and 17.87°C in the third day.

- 1<sup>st</sup> Day measurements

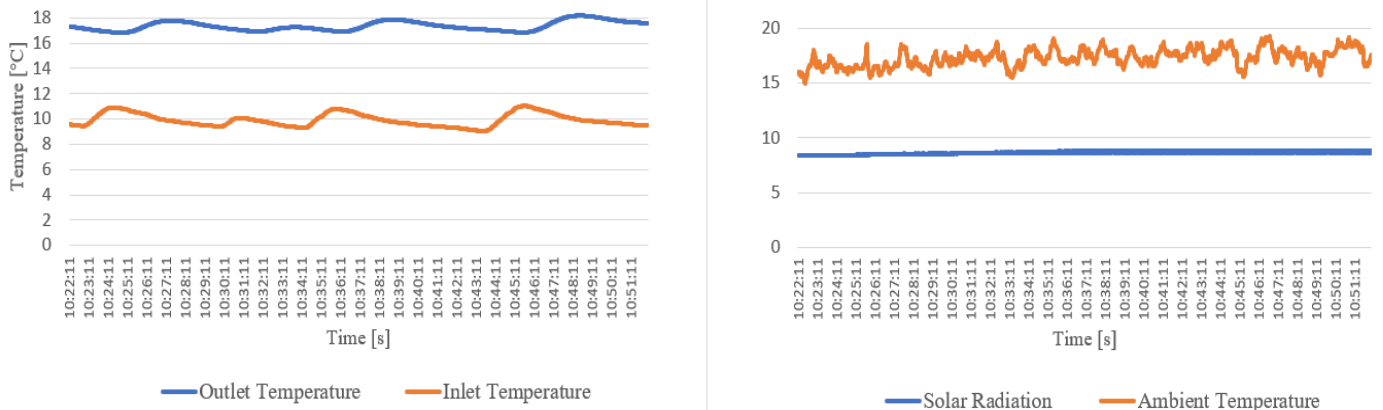


**Figure 35.** The outlet, inlet and ambient temperature in function of time under (1040-1170W/m<sup>2</sup>) (1<sup>st</sup> Day)

**Table 17.** The average of the ambient, inlet and the outlet temperature (1040-1170W/m<sup>2</sup>) (1<sup>st</sup> Day)

| Avg. Solar irradiation [W/m <sup>2</sup> ] | Ambient Temperature [°C] | Inlet Temp [°C] | Outlet Temp [°C] |
|--|--------------------------|-----------------|------------------|
| 1120.6                                     | 17.30                    | 9.92            | 17.35            |

- 2<sup>nd</sup> Day measurements

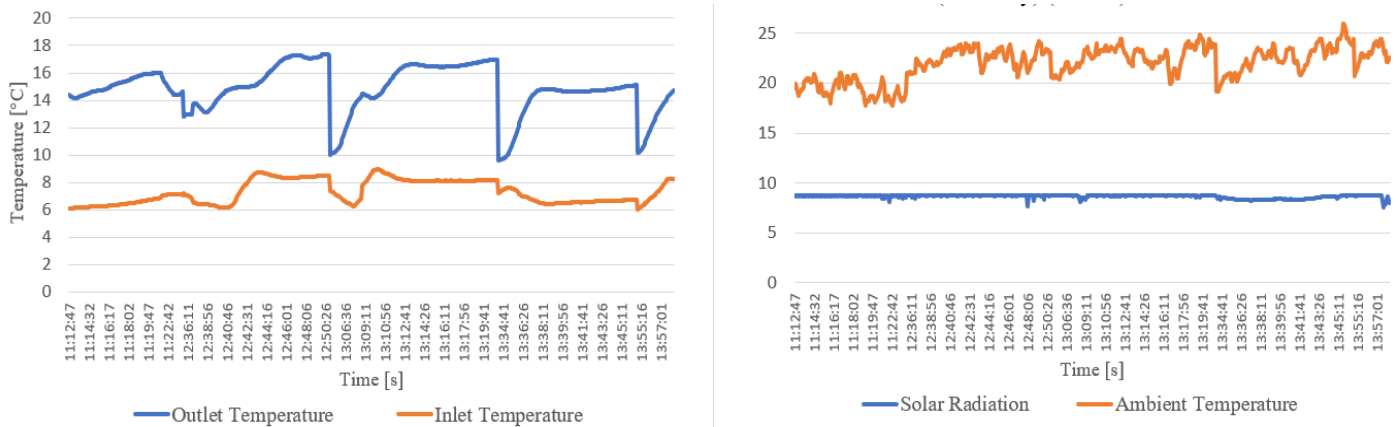


**Figure 36.** The outlet, inlet and ambient temperature in function of time under (1040-1170W/m<sup>2</sup>) (2<sup>nd</sup> Day)

**Table 18.** The average of the ambient, inlet and the outlet temperature (1040-1170W/m<sup>2</sup>) (2<sup>nd</sup> Day)

| Avg. Solar irradiation [W/m <sup>2</sup> ] | Ambient Temperature [°C] | Inlet Temp [°C] | Outlet Temp [°C] |
|--|--------------------------|-----------------|------------------|
| 1127.1                                     | 22.00                    | 7.31            | 14.82            |

- 3<sup>rd</sup> Day measurements

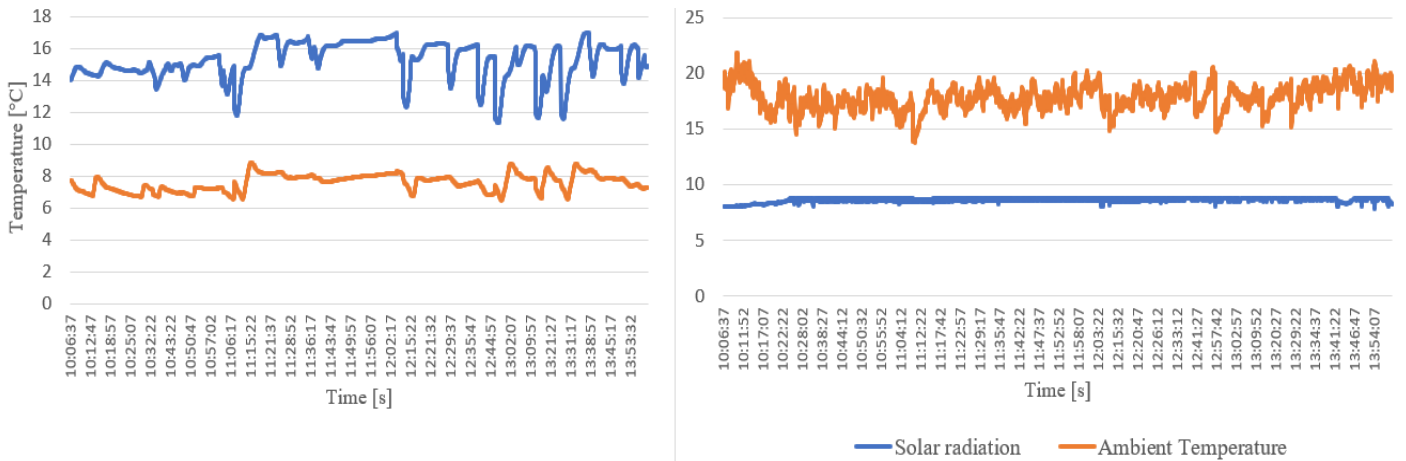


**Figure 37.** The outlet, inlet and ambient temperature in function of time under (1040-1170W/m<sup>2</sup>) (3<sup>rd</sup> Day)

**Table 19.** The average of the ambient, inlet and the outlet temperature (1040-1170W/m<sup>2</sup>) (3<sup>rd</sup> Day)

| Avg. Solar irradiation [W/m <sup>2</sup> ] | Ambient Temperature [°C] | Inlet Temp [°C] | Outlet Temp [°C] |
|--|--------------------------|-----------------|------------------|
| 1121.9                                     | 17.87                    | 7.57            | 15.21            |

### 4.3 The extracted heat and coefficient of performance (COP)

In this study I focused more on the preparation of the outlet temperature of solar collector, therefor in how to increase the extracted heat from the solar collector that will be the heat source of the heat pump in the other half of the system, during the experiments there was an instantly measure of the consumed current by the heat pump compressor, therefore the consumed power. The COP can be calculated using the following formula:

$$COP = \frac{Q_{0.avg} + P_{eff.avg}}{P_{eff.avg}} \quad (19)$$

Where:

$Q_0$  The obtained heat from the solar collector [W] can be calculated by using the formula number (7).

$P_{eff.avg}$  The power consumed by the compressor [W] can be calculated using the following formula:

$$P_{eff} = U_{eff} \cdot I_{eff} \quad (20)$$

Where:

$U_{eff}$  the voltage from the grid usually 230 V

$I_{eff}$  the consumed current by the compressor [A]

- 1<sup>st</sup> Day measurements

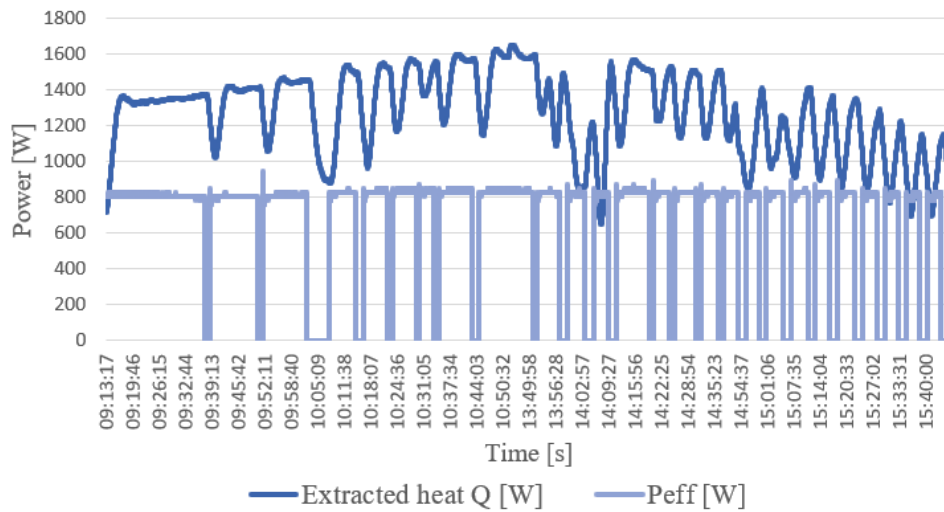


**Figure 38.** Extracted heat and the consumed power by the heat pump compressor during the 1<sup>st</sup> day

The results from Figure 38 shows that the extracted heat from the solar collector varies between 800W and 1600 W, where we can notice that the compressor is changing phase from ON to OFF when the extracted heat by the solar collector drops down to a certain value of power (around 800W), and during the ON phase the consumed power by the compressor does not usually exceed 800 W. As it is shown in table 20 the average COP during the first day is 2.80 that can be demonstrated by the system’s beneficitation from the continues extracted heat from the solar collector to heat up the tank when the heat pump cycle is OFF.

**Table 20.** The average value of the extracted heat, consumed power and COP (1<sup>st</sup> day)

| Avg. $Q_0$ [W] | Avg. $P_{eff}$ [W] | Avg. COP |
|----------------|--------------------|----------|
| 1252.46        | 695.16             | 2.80     |

- 2nd Day measurements

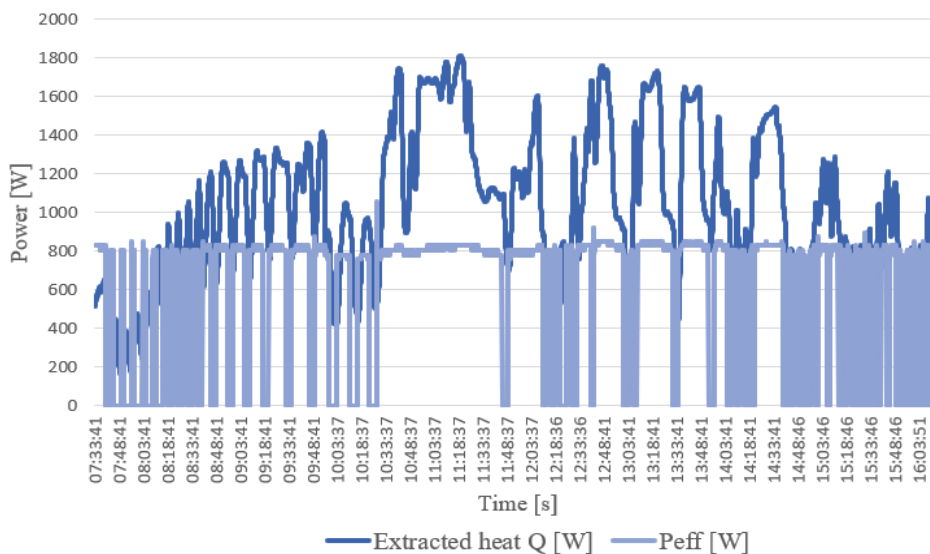


**Figure 39.** Extracted heat and the consumed power by the heat pump compressor during the 2<sup>nd</sup> day

**Table 21.** The average value of the extracted heat, consumed power and COP (2<sup>nd</sup> day)

| Avg. $Q_0$ [W] | Avg. $P_{eff}$ [W] | Avg. COP |
|----------------|--------------------|----------|
| 1013.92        | 575                | 2.76     |

From Figure 39 we can notice that the extracted heat from the solar collector during the early morning of the second day was less than the power consumed by the compressor and after 9:00 am, start varies between 800W and 1700 W, where the consumed power by the compressor is changing phase from ON to OFF when the extracted heat by the solar collector drops down to a certain value of power (around 600W in this case). During the ON phase the consumed power by the compressor does not usually exceed 850 W in this case. As it is shown in table 21 the average of the consumed power by the compressor is around 575W that the OFF phase is repeated and sometimes stay longer, the COP during the second day is 2.76 less than the first Cop that can be demonstrated by the cloudy nature of the 3<sup>rd</sup> Day weather.

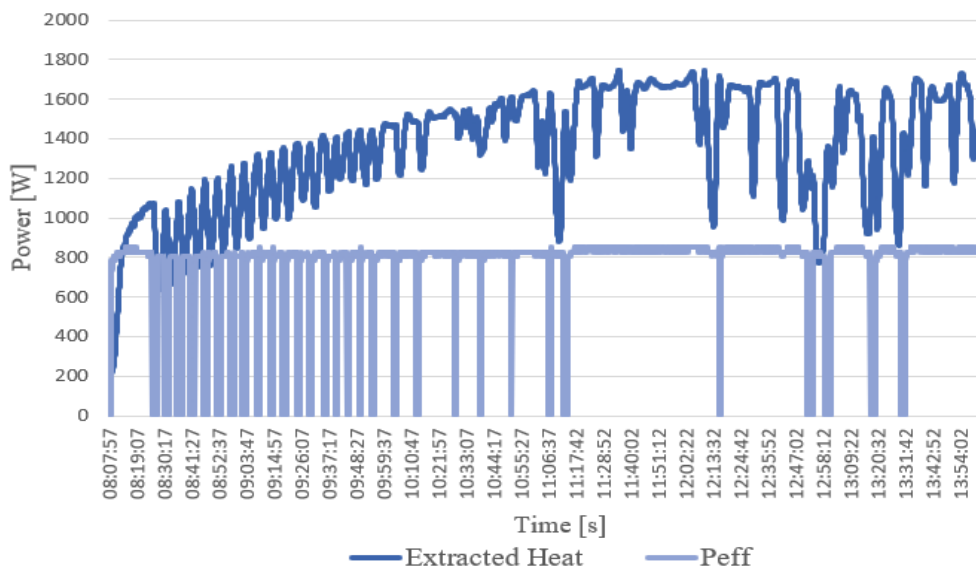


**Figure 40.** Extracted heat and the consumed power by the heat pump compressor during the 3<sup>rd</sup> day

The results from Figure 40 shows that the Extracted heat from the solar collector varies between 900W and 1700 W during the third day, where we can notice that the compressor is changing phase from ON to OFF when the extracted heat by the solar collector drops down to a certain value of power (around 900-1000W), and during the ON phase the consumed power by the compressor does not usually exceed 850 W. As it is shown in table 22 the average COP during the first day is 2.86 that can be demonstrated by the system's beneficitation from the continues extracted heat from the solar collector to heat up the tank when the heat pump cycle is OFF, as well as the good availability of the solar irradiation where the average solar irradiation in the third day was around 921.07W/m<sup>2</sup> therefore we have more significant heat extracted during the third day.

**Table 22.** The average value of the extracted heat, consumed power and COP (3<sup>rd</sup> day)

| Avg. $Q_0$ [W] | Avg. $P_{eff}$ [W] | Avg. COP |
|----------------|--------------------|----------|
| 1354.55        | 727.91             | 2.86     |



#### 4.4 MATLAB Simulink Results

The combination of MATLAB simulation results with the experiments results may help investigate system performance and highlight the gaps our system contains.

- 1<sup>st</sup> Day measurements

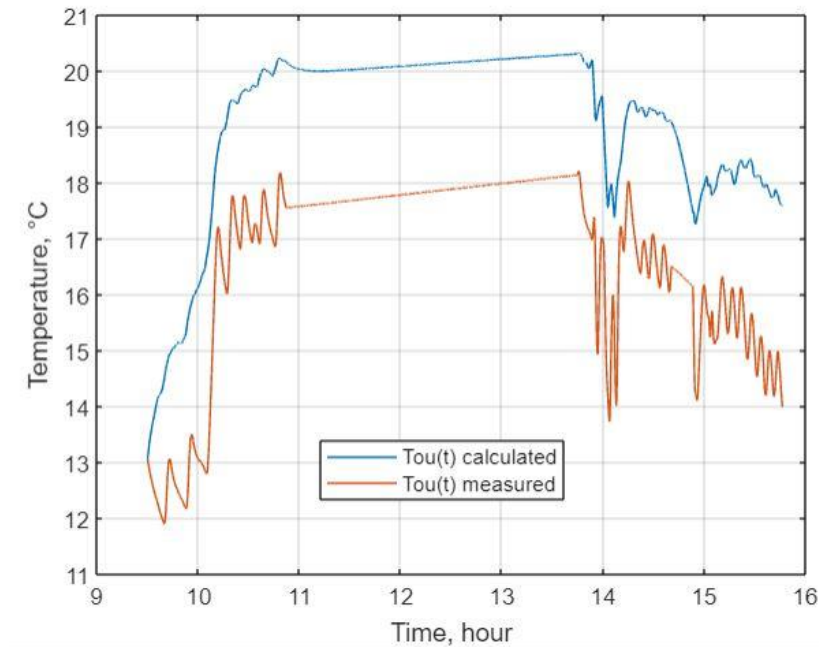


**Figure 41.** The measured and simulated outlet temperature by MATLAB Simulink (1<sup>st</sup> day)

- 2<sup>nd</sup> Day measurements

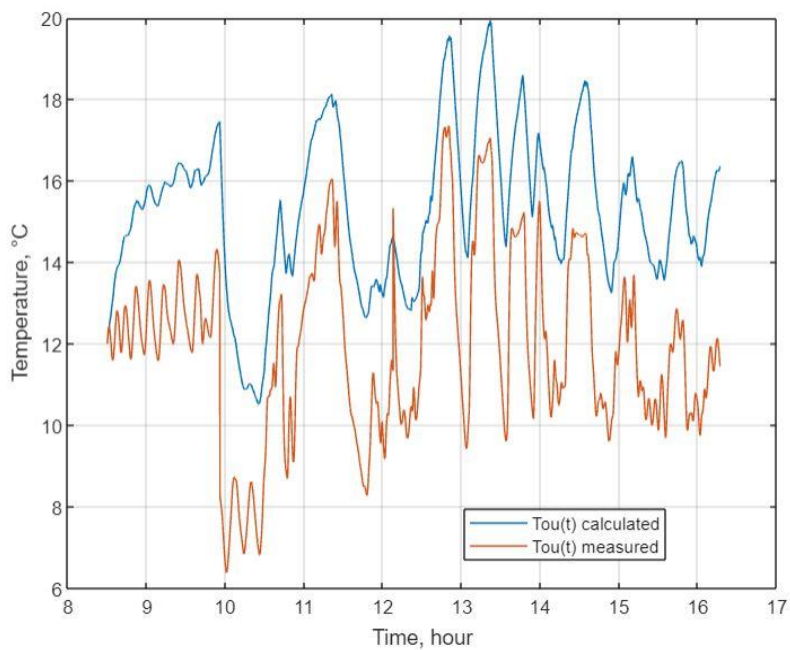


**Figure 42.** The measured and simulated outlet temperature by MATLAB Simulink (2<sup>nd</sup> day)



- 3<sup>rd</sup> Day measurements

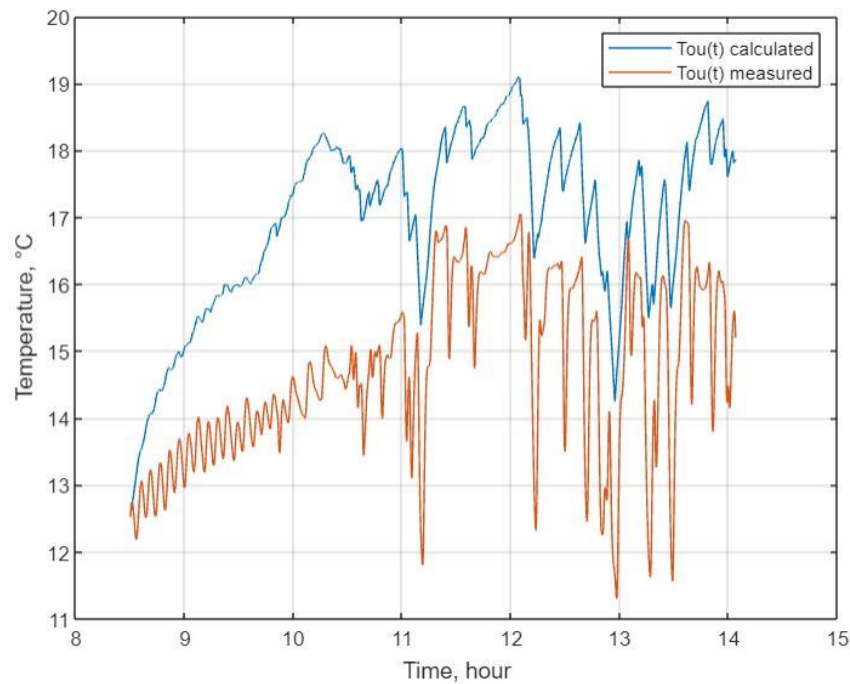


**Figure 43.** The measured and simulated outlet temperature by MATLAB Simulink (2<sup>nd</sup> day)

The results from the Figure 41, Figure 42 and Figure 43 shows that for same initial conditions the change in the calculated outlet temperature of the solar collector by MATLAB Simulink is changing approximately in same way as the measured values with (+2 to 3 °C) of difference, As the Simulink values predict in all cases an outlet temperature that's is greater than the measured values and we can demonstrate this difference with the following assumptions.

- In the real measurements the position of the position of temperature sensors in the inlet and outlet of the solar collector was 4 meters far from the exact outlet and inlet of the solar collector.
- The bad insulation of the pipes in the whole system.
- MATLAB model may not be accurate for this temperature ranges.

The other thing that can be noticed from the MATLAB results, there is always a time lag between the measured and the calculated outlet temperature that could be acceptable if we consider that the Simulink model check first if the pump is On or Off, where in the real case it works in a more instantly way.

#### 4.5 Comparisons with previous works

The current results concerning the strong effect of solar irradiation on the performance of the solar collector have been verified by multiple other researchers, Elmetwalli et al. (2022) found that higher solar radiation results in more significant heat gain and vice versa. Simonetti et al. (2019) created a novel PV/T dual source evaporator, the results demonstrate that solar irradiation has a substantial impact on the SAHP system's performance and that this system has a 14% higher COP than a typical air source heat pump.

A.H. Elmetwalli et al. (2022)'s research came up with the importance of the ambient air temperature surrounding the solar collector systems that it is one of the main factors affecting the heat gain or loss of water inside the storage tank where I found that the ambient temperature has a slight effect in front of the solar irradiation, but still, in my case, I can always benefit from the ambient temperature during the absence of solar irradiation, that the heat extracted from the solar collector is the heat source of the heat pump where the refrigerant using the low-temperature ranges. The usage of the ambient temperature as the heat source of the heat pump when the absence of solar radiation makes the system under the name double source solar assisted heat pump and further research demonstrates that the dual heat source mode's heating capacity improves by 62% and its coefficient of performance (COP) rises by 59% when compared to the single air heat source mode (Liu et al., 2016).

The influence of the inlet temperature is not taken into consideration before in other research in the same way as it is figured out in my results, where the current results show that when the more the inlet temperature is low, the more significant the extracted heat by the solar collector will be.

## 5 Conclusion

The impact of changing the inlet temperature of the solar collector under same solar irradiation conditions over three days of experiments was the first goal of my work, in order to evaluate the amount of the heat that can be extracted in low inlet temperature ranges. Under variable ambient temperature during three days, and fixed inlet temperature I also measured the change of the outlet temperature in same solar radiation range. In another way observing the resultant outlet temperature during the same range of solar irradiation and approximately same ambient temperature where the inlet temperature is taking different values in each of the three days. The experiments have been done in Gödöllő city in Hungary, for three days 12, 23, and 26 April 2023. The study of the system has been conducted using experimental data and a MATLAB Simulink model. The most important remarking points have been listed:

- (1) In high solar irradiation ranges the extracted heat by the heat transfer medium is more significant when the inlet temperature is low.
- (2) During the experiments it was noticed that the amount of increase in the outlet temperature is more significant when the inlet temperature is much low than when it is close to the ambient temperature.
- (3) That is very useful in the heat pump systems with a storage tank, where is known the refrigerant is working with low-temperature ranges therefore, it is more significant to heat up the heat transfer medium circulating inside the collector from  $-5^{\circ}\text{C}$  to  $0^{\circ}\text{C}$ , than from  $+30$  to  $+33^{\circ}\text{C}$ . The storage tank is added to the system to increase the efficiency of solar energy usage and increase operating time.
- (4) Solar irradiation has a strong and direct effect on the variation of the outlet temperature of the solar collector.
- (5) When the absence of solar irradiation the heat pump system can be assisted by the ambient temperature as a heat source making a double source solar-assisted heat pump.
- (6) In high solar irradiation ranges (in my experiments) the ambient temperature has a neglected effect on increasing the outlet temperature of the solar collector.

To advance the state of knowledge regarding this topic, the following future research is suggested to enhance this study:

- (1) Look for correlations to determine the optimum interconnection parameters for solar panels, collectors, and heat pump systems, focusing more on energy storage issues, taking into consideration that battery banks and thermal storage are promising components for improving energy conservation and reliability of power systems.
- (2) Research limitations on exergy analysis. The exergy analysis evaluates the efficient use of solar energy by calculating the sources and magnitude of irreversibility; consequently, this analysis can be used to enhance the performance of the system, particularly the PV/T-assisted heat pump system.
- (3) Developing the optimal operation control strategies, that could aim to reduce the cost of investments, and life cycle costs.
- (4) Adding other renewable energy sources, such as wind energy and biomass energy, to enhance the efficiency of the systems (double or more source solar assisted heat pump).

## 6 Summary

The recent gas crisis has highlighted the importance of alternative sources of energy for heating and cooling homes and buildings. One promising technology that can help reduce reliance on fossil fuels is the solar-assisted heat pump (SAHP). SAHP systems combine solar energy with heat pump technology to provide efficient and sustainable heating and cooling solutions. Bas well as reducing energy bills and lower carbon emissions, making them an attractive option for homeowners and businesses. The work presented aims to construct a double-source solar-assisted heat pump (solar energy and ambient temperature) with a storage tank and investigate the impact of controlling the inlet temperature by comparing the results of the solar collector's outlet temperature under identical solar irradiance conditions and the same mass flow of the heat transfer medium over three days. Therefore, my hypothesis is that the lower the temperature of the heat transfer medium entering the collector, the greater the efficiency of the system, resulting in a greater amount of extracted heat to assist the heat pump evaporator over a longer period of time, where the refrigerant in the heat pump side is working with low-temperature ranges, therefore, to heat up a circulated fluid from  $-5\text{ }^{\circ}\text{C}$  to  $0^{\circ}\text{C}$  is more degrees will be much significant than heating up a high-temperature fluid.

The execution of the system was carried out at the energetic building's laboratory of the Hungarian University of Agriculture and Life Sciences. The main component of the system is the heat pump which is assisted by a flat plate solar collector placed outside on the roof of the mentioned building, forming two main circuits the antifreeze circuit and the refrigerant circuit; in this study, I am going to focus on the antifreeze circuit where the investigation of the change of the outlet temperature in function of external conditions and the inlet temperature of the solar collector. The experiments take place over three days, in each day we set different inlet temperatures of the solar collector and we see how the outlet temperature is changing in almost the same values of solar radiation in each day. In the experiments we also investigate the change of the extracted heat according to the inlet temperature and the external conditions during the day, then the coefficient of performance of the whole system including the heat pump, the heat pump during the whole system running period change phase ON/OFF, when the inlet temperature drops below the fixed value, the heat pump shuts off, the start of the next heat pump cycle will be when the inlet temperature reaches again the previously set temperature point. Therefore, the tank during the OFF phase of the heat pump continues charging by the solar collector increasing by that the performance of the system.

A digital thermostat was used to control the inlet temperature during the day. The thermostat was equipped with a temperature's sensors to measure the outlet and inlet temperature, both of them were connected to the ALMEMO system in order to instantly record the collected data. The ambient temperature, solar irradiation and the instantly consumed current in the compressor were also measured during the experiments and recorded in the ALMEMO system in order to calculate the COP of the whole system.

The obtained results after analyzing the data record:

- (1) In high solar irradiation ranges the extracted heat by the heat transfer medium is more significant when the inlet temperature is low.

- (2) During the experiments it was noticed that the amount of increase in the outlet temperature is more significant when the inlet temperature is much low than when it is close to the ambient temperature.
- (3) That is very useful in the heat pump systems with a storage tank, where is known the refrigerant is working with low-temperature ranges therefore, it is more significant to heat up the heat transfer medium circulating inside the collector from  $-5^{\circ}\text{C}$  to  $0^{\circ}\text{C}$ , than from  $+30$  to  $+33^{\circ}\text{C}$ . The storage tank is added to the system to increase the efficiency of solar energy usage and increase operating time.
- (4) Solar irradiation has a strong and direct effect on the variation of the outlet temperature of the solar collector.
- (5) When the absence of solar irradiation the heat pump system can be assisted by the ambient temperature as a heat source making a double source solar-assisted heat pump.
- (6) In high solar irradiation ranges (in my experiments) the ambient temperature has a neglected effect on increasing the outlet temperature of the solar collector.

To simulate the outlet temperature of the solar collector change under the measured external condition and the measured inlet temperature of the solar collector, MATLAB Simulink software was used, The obtained results from the MATLAB calculation shows that for the same initial conditions, the change in the calculated outlet temperature of the solar collector by MATLAB Simulink is changing approximately in the same way as the measured values with (+2 to 3 °C) of difference, As the Simulink values predict in all cases an outlet temperature that's is greater than the measured values and we can demonstrate this difference with the following assumptions.

- In the real measurements the position of the position of temperature sensors in the inlet and outlet of the solar collector was 4 meters far from the exact outlet and inlet of the solar collector.
- The bad insulation of the pipes in the whole system.
- MATLAB model may not be accurate for this temperature range.

To advance the state of knowledge regarding this topic, the following future research is suggested to enhance this study:

- (1) Look for correlations to determine the optimum interconnection parameters for solar panels, collectors, and heat pump systems, focusing more on energy storage issues, taking into consideration that battery banks and thermal storage are promising components for improving energy conservation and reliability of power systems.
- (2) Research limitations on exergy analysis. The exergy analysis evaluates the efficient use of solar energy by calculating the sources and magnitude of irreversibility; consequently, this analysis can be used to enhance the performance of the system, particularly the PV/T-assisted heat pump system.
- (3) Developing the optimal operation control strategies, that could aim to reduce the cost of investments, and life cycle costs.
- (4) Adding other renewable energy sources, such as wind energy and biomass energy, to enhance the efficiency of the systems (double or more source solar assisted heat pump).

## DECLARATION

### on authenticity and public assess of final master's thesis

Student's name: Hasna Saadi  
Student's Neptun ID: XTNU6K  
Title of the document: Solar energy utilization with the heat pumps  
Year of publication: 2023  
Department: Mechanical Engineering

I declare that the submitted master's thesis is my own, original individual creation. Any parts taken from an another author's work are clearly marked, and listed in the table of contents.

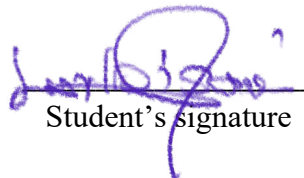
If the statements above are not true, I acknowledge that the Final examination board excludes me from participation in the final exam, and I am only allowed to take final exam if I submit another master's thesis.

Viewing and printing my submitted work in a PDF format is permitted. However, the modification of my submitted work shall not be permitted.

I acknowledge that the rules on Intellectual Property Management of Hungarian University of Agriculture and Life Sciences shall apply to my work as an intellectual property.

I acknowledge that the electric version of my work is uploaded to the repository sytem of the Hungarian University of Agriculture and Life Sciences.

Place and date: Gödöllő, 2023 May 09

  
Student's signature

## STATEMENT ON CONSULTATION PRACTICES

As a supervisor of Hasna Saadi XTNU6K, I here declare that the master's thesis has been reviewed by me, the student was informed about the requirements of literary sources management and its legal and ethical rules.

**I recommend**/don't recommend master's thesis to be defended in a final exam.

The document contains state secrets or professional secrets: yes     **no**

Place and date: Gödöllő, 2023 May 09



---

Internal supervisor

## References

- Amo AD., Martínez-Gracia A, et al. (2019), Performance analysis and experimental validation of a solar-assisted heat pump fed by photovoltaic-thermal collectors, *Energy*, 169:1214–23.
- Bakirci K, Yuksel B, et al. (2011), Experimental thermal performance of a solar source heat-pump system for residential heating in cold climate region, *Appl Therm Eng*, 31(8–9):1508–18s.
- Bai Y, Chow TT, Menezo C, et al. (2012), Analysis of a hybrid PV/thermal solar-assisted heat pump system for sports center water heating application, *Int J Photoenergy*, 2012;1:1022–3.
- Cai J, Ji J, Wang Y, Huang W. (2017), Operation characteristics of a novel dual source multi-functional heat pump system under various working modes, *Appl Energy*, 194:236–46.
- Caglar A, Yamali C. (2012), Performance analysis of a solar-assisted heat pump with an evacuated tubular collector for domestic heating, *Energy Build*, 54:22–8.
- Cai J, Li Z, Ji J, Zhou F. (2019), Performance analysis of a novel air source hybrid solar assisted heat pump, *Renewable Energy*, 139:1133–45.
- Cardemil JM, Schneider W, Behzad M, et al. (2020), Thermal analysis of a water source heat pump for space heating using an outdoor pool as a heat source, *Journal of Building Engineering*, 33:101581.
- Defra Report, (2008) Measurement of Domestic Hot Water Consumption in Dwellings, Defra Rep, 2008,pp.1e62.
- Deng W., Yu J., Simulation analysis on dynamic performance of a combined solar/ air dual source heat pump water heater, *Energy Convers, Manag*, 120 378–387, <https://doi.org/10.1016/j.enconman.2016.04.102>.
- Dikici A, Akbulut A. (2008), Performance characteristics and energy-exergy analysis of solar-assisted heat pump system, *Build Environ*, 43(11):1961–72.
- Dannemand M, Perers B, Furbo S. (2019) Performance of a demonstration solar PVT assisted heat pump system with cold buffer storage and domestic hot water storage tanks, *Energy Build*, 188:46–57.
- Emmi G, Zarrella A, Carli MD, et al. (2015) An analysis of solar-assisted ground source heat pumps in cold climates. *Energy Convers Manage*,106:660–75.
- Elmetwalli A.H., Darwesh M.R., Amer M.M., M.S. Ghoname. (2022), Influence of solar radiation and surrounding temperature on heating water inside solar collector tank, *Journal of Energy Storage*, 47 103648.
- Freeman J., Guarracino I., Kalogirou S.A., Markides C.N. (2017), A small-scale solar organic Rankine cycle combined heat and power system with integrated thermal energy storage, *Appl. Therm. Eng.* 127 1543e1554, <https://doi.org/10.1016/j.applthermaleng.2017.07.163>.
- Hüsing F., Hirsch., H., Rockendorf G. (2016), Combination of solar thermal collectors and horizontal ground heat exchangers as optimized source for heat pumps, *International solar energy society, Conference proceedings Eurosun*.



IEA. Transition to Sustainable Buildings. 2013 21.08.2020]; Available from: <https://www.iea.org/reports/transition-to-sustainable-buildings>.

IEA. World Energy Outlook [Online]. 2019 21.08.2020]; Available from: <https://www.iea.org/weo2019/>.

Jinping Li., Chaofan Qu., Caijun Li., Xiaomin Liu. (2022), Vojislav Novakovic (2022), Technical and economic performance analysis of large flat plate solar collector coupled air source heat pump heating system, *Energy & Buildings* 277 112564.

Kutlu C, Zhang Y, Elmer T, et al. (2020), A simulation study on performance improvement of solar assisted heat pump hot water system by novel controllable crystallization of supercooled PCMs. *Renewable Energy*, 152:601–12.

Khan Z, Khan Z, Ghafoor A. (2016), A review of performance enhancement of PCM-based latent heat storage system within the context of materials, thermal stability, and compatibility, *Energy Convers Manage*, 2016;115:132–58.

Kousksou T., Bruel P., Cherreau G., Leoussoff V., El Rhafiki T., PCM storage for solar DHW, from an unfulfilled promise to a real benefit, *Sol. Energy*, 85-2033e2040, <https://doi.org/10.1016/j.solener.2011.05.012>.

Li H., Yang H. (2010) Study on performance of solar assisted air source heat pump systems for hot water production in Hong Kong, *Appl, Energy* 87 2818–2825, <https://doi.org/10.1016/j.apenergy.2009.06.023>.

Liu Y, Ma J, Zhou G, Zhang C, Wan W. (2016), Performance of a solar air composite heat source heat pump system. *Renewable Energy*, 2016;87:1053–8.

Liang C.H., Zhang X.S., Li X.W., Zhu X. (2011), Study on the performance of a solar assisted air source heat pump system for building heating, *Energy Build*, 43-2188–2196.

Mehling H., Cabeza L.F., Hippeli S., Hiebler S. (2003), PCM-module to improve hot water heat stores with stratification, *Renew. Energy* 28 699e711.

Makoto T. (2008), Regional report asia and pacific, in: 9th International IEA Heat Pump Conference, Zurich, Switzerland, May 20-22.

Mark D., Ioannis S., Zhiyong T., Simon F. (2020), *Energy Conversion and Management*, 206 (2020) 112429

Ni L., Qv D., Shang R., Yao Y., Niu F. (2016), W. Hu, Experimental study on performance of a solar-air source heat pump system in severe external conditions and switchover of different functions, *Sustain. Energy Technol. Assessments*, 16 162–173, <https://doi.org/10.1016/j.seta.2016.06.001>.

Nouri G. (2019), Designing and optimization of solar-assisted ground source heat pump system to supply heating, cooling, and hot water demands, *Geothermics* 82: 212–31

Nuntaphan A, Chansena C, Kiatsiriroat T. (2009), Performance analysis of solar water heater combined with heat pump using refrigerant mixture, *Appl Energy*, 86 (5):748–56.

- Ozgener O., Hepbasli A., (2005), Performance analysis of a solar-assisted ground-source heat pump system for greenhouse heating: an experimental study, *Build Environ*, 40(8):1040–50.
- Philippen D., Battaglia M., Carbonell D., Thissen B., Kunath L. (2018), Validation of an Ice Storage Model and its Integration into a Solar-Ice System, *International Solar Energy Society EuroSun 2018 Conference Proceedings*.
- Panaras G., Mathioulakis E., Belessiotis V. (2014), A method for the dynamic testing and evaluation of the performance of combined solar thermal heat pump hot water systems, *Appl Energy*, 114:124–34.4
- Ran SY., Li XT., Xu W., et al. (2020), A solar-air hybrid source heat pump for space heating and domestic hot water, *Sol Energy*, 199:347–59.
- Si P., Li .A, Rong X., et al. (2015), New optimized model for water temperature calculation of river-water source heat pump and its application in simulation of energy consumption, *Renewable Energy*, 84:65–73.
- Sporn, P., Ambrose, E.R. (1955), The heat pump and solar energy, *Proceed World Symposium on Appl, Solar Energy*, pp. 1–5
- Sterling SJ., Collins MR. (2012), Feasibility analysis of an indirect heat pump assisted solar domestic hot water system, *Appl Energy* , 93(5):11–7.
- Si Q., Okumiya M., Zhang XS. (2014), Performance evaluation and optimization of a novel solar-ground source heat pump system, *Energy Build*, 70:237–45.
- Sezen K, Tuncer A, Akyuz A, et al. (2021), Effects of ambient conditions on solar assisted heat pump systems, *A review Sci Total Environ*, 778:146362.
- Simonetti R., Molinaroli L., Manzolini G. (2019), Experimental and analytical study of an innovative integrated dual-source evaporator for solar-assisted heat pumps, *Sol Energy*, 194:939–51.
- Stojanovi B., Akander J. (2010), Build-up and long-term performance test of a full-scale solar-assisted heat pump system for residential heating in Nordic climatic conditions, *Appl Therm Eng*, 30:188–95.
- Trillat-Berdal V., Souyri B., Fraisse G. (2006), Experimental study of a ground-coupled heat pump combined with thermal solar collectors, *Energy Build*, 38(12): 1477–84.
- Talmatsky E., Kribus A. (2008), PCM storage for solar DHW: an unfulfilled promise? *Sol. Energy* 82 861e869, <https://doi.org/10.1016/j.solener.2008.04.003>
- Wang Y., Li M., Qiu Y., et al. (2019), Performance analysis of a secondary heat recovery solar-assisted heat pump drying system for mango. *Energy Explor Exploit*.
- Wang G, Zhao YH, Quan ZH, et al. (2018), Application of a multi-function solar-heat pump system in residential buildings. *Applied thermal engineering: Design, processes, equipment, economics* 130:992–1937.
- Wang Y., Quan Z., Zhao Y., Wang L., Liu Z. (2022), Performance and optimization of a novel solar-air source heat pump building energy supply system with energy storage *Applied Energy*, 324 (2022) 119706.

- Wang Y., Rao Z., Liu J., Liao S. (2020), An optimized control strategy for integrated solar and air-source heat pump water heating system with cascade storage tanks, *Energy Build*, 210 109766, <https://doi.org/10.1016/j.enbuild.2020.109766>.
- Wang X., Xia L., Bales C., et al. (2020), A systematic review of recent air source heat pump (ASHP) systems assisted by solar thermal, photovoltaic and photovoltaic/thermal sources. *Renewable Energy* 146(2):2472–87.
- Winteler C., Dott R., Afjei T., Hafner B. (2014), Heat pump, solar energy and ice storage systems - modelling and seasonal performance, hIEA Heat Pump Conference, 12-16 2014, Poster P.3.12.
- Yerdesh Y., Abdulina Z., Aliuly A., Belyayev Y., Mohanraj M., Kaltayev A. (2020), Numerical simulation on solar collector and cascade heat pump combi water heating systems in Kazakhstan climates, *Renew. Energy* 145 1222e1234, <https://doi.org/10.1016/j.renene.2019.06.102>.
- Yumrutas R., Kaska O. (2004), Experimental investigation of thermal performance of a solar assisted heat pump system with an energy storage, *Int J Energy Res*,28 (2):163–75.
- Youssef W., Ge YT., Tassou SA. (2017), Effects of latent heat storage and controls on stability and performance of a solar assisted heat pump system for domestic hot water production. *Sol Energy* 150(38092X):394–407.
- Yang W., Sun L., Chen Y. (2015), Experimental investigations of the performance of a solar-ground source heat pump system operated in heating modes, *Energy Build*, 89:97–111.
- Zhou J., Zeng C., Wang Z., Lyu W., Tang Y., Wu D., Wenhui J., Yanping Y. (2022), Sustainable Energy Technologies and Assessments Indirect expansion solar assisted heat pump system, A review 53-102409.
- Zhang X., Zhao X., Shen J., et al. (2013), Design, fabrication and experimental study of a solar photovoltaic/loop-heat-pipe based heat pump system, *Sol Energy* 97: 551–68.

# Appendix

## Appendix 1. Si Global Radiation Sensor



6003.0000 BG

### Si Global Radiation Sensor

GROUP 6



RADIATION

NO

6003.0000

VERSION / DATE

04 / 03 2015

#### Connection plan

2.5 m on fixed cable:

##### Version 6003.1000, 0...5 V

|   |       |                 |
|---|-------|-----------------|
| 1 | white | Supply Vcc / Ua |
| 2 | brown | GND             |
| 3 | green | Signal GS       |

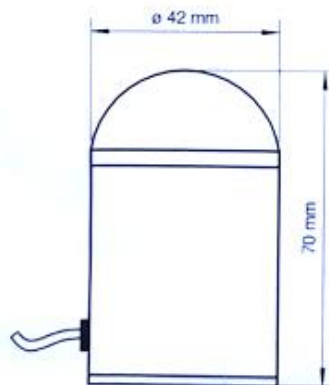
##### Version 6003.2000, 4 ... 20 mA

|   |       |                 |
|---|-------|-----------------|
| 1 | white | Supply Vcc / Ua |
| 2 | brown | GND             |

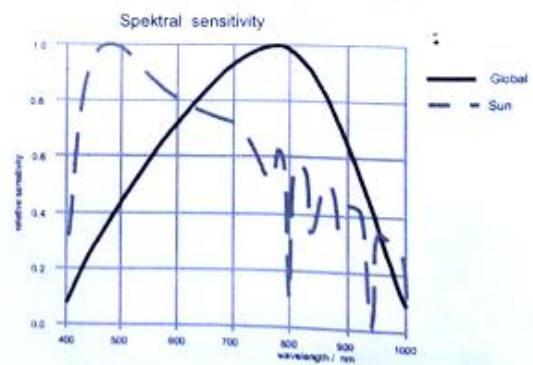
##### Version 6000.3000, 0 ... 10 V

|   |        |                 |
|---|--------|-----------------|
| 1 | white  | Supply Vcc / Ua |
| 2 | brown  | GND             |
| 3 | grey   | GND             |
| 3 | yellow | Output          |

#### Dimensions



#### Diagram



Technical data are subject to change!



## Si Global Radiation Sensor

GROUP 6

RADIATION

NO.

**6003.0000**

VERSION / DATE / NAME 04 / 03.2015 / KI



### Description

The Sensor measures the global radiation, basing on a silicon diode with diffusor and PMMA-dome. Especially suitable as reference for photovoltaic systems, including built-in measuring amplifier.

The measuring results are allowing conclusions about medical and biological connections comparing to other spectral ranges.

The measuring head can be used in medical and biological research, in weather information and forecast systems, in climate research, in the agriculture and for public information in general.

### Technical Data

|                      |                            |                      |                     |
|----------------------|----------------------------|----------------------|---------------------|
| Meas. Range:         | 0...1.300 W/m <sup>2</sup> |                      |                     |
| Spectr. Sensitivity: | 380 nm...1.100 nm          |                      |                     |
| max. Sensitivity at: | 780 nm                     |                      |                     |
| Operating Temp.:     | -20... +60 °C              |                      |                     |
| Output:              | 6003.1000: 0...5 V         | 6003.2000: 4...20 mA | 6003.3000: 0...10 V |
| Power Supply:        | 9...30 VDC                 |                      |                     |
| Diffusor:            | PTFE                       |                      |                     |
| Dome:                | PMMA (UV- pervious)        |                      |                     |
| Cosinus Correction:  | f2 < 6 %                   |                      |                     |
| Linearity:           | 6003.1000: < 5 %           | 6003.2000: < 5 %     | 6003.3000: < 3 %    |
| Absolute Error:      | < 10 %                     |                      |                     |
| Dimensions:          | Ø 42 x 70 mm               |                      |                     |
| Weight:              | approx. 100 g              |                      |                     |

### Ordering Code

|                             |                  |                  |
|-----------------------------|------------------|------------------|
| Si-Global Radiation Sensor, | output 0...5 V   | <b>6003.1000</b> |
| Si-Global Radiation Sensor, | output 4...20 mA | <b>6003.2000</b> |
| Si-Global Radiation Sensor  | output 0...10 V  | <b>6003.3000</b> |

Technical data are subject to change!

## Appendix2. Parameter file and Data file required for the simulation (M-file) (1<sup>st</sup> Day)

```
% Simulate the Simulink model of the flat-plate solar collector
% and plot the measured and calculated temperatures
% MATLAB code file name: run_sol_coll.m
% Parameters and hot water extraction function for modelling and simulation
% a flat-plate solar collector
% MATLAB code file name: collp2.m
%% By: Dr. János BUZÁS
% Hasna Saadi
% Department of Mechatronics, Institute of Technology
% Hungarian University of Agriculture and Life Sciences
% April 26, 2023
Ac = 1.92; % collector absorber surface, m^2
eta= 0.80; % optical efficiency of the collector,(dimensionless)
roc= 1050; % density of the collector heat transfer medium, kgm-3
% (A 1:1 mixture of propylene glycol and distilled water)
cc = 3600; % specific heat of the collector heat transfer medium, Jkg-1K-1
Vc = 0.025; % volume of heat transfer medium in the collector, m^3
C =roc*cc*Vc; % heat capacity of the heat transfer medium in the collector, JK-1
Ul = 35; % total heat loss factor of the collector, Wm-2K-1
vc = 4.9166e-5; % volume flow of the collector circuit, m^3 s-1

Data Matrix U= [.....];

% Simulate the Simulink model of the flat-plate solar collector
% and plot the measured and calculated temperatures
% MATLAB code file name: run_sol_coll.m
% The name of the MATLAB Code file containing the parameters of the Simulink model: collp2.m
% The file containing the measured data matrix for the simulation: s1990503.m
% The name of the Simulink model file: sol_coll.slx
%% By: Dr. János BUZÁS
% Hasna Saadi
% Department of Mechatronics, Institute of Technology
% Hungarian University of Agriculture and Life Sciences
% April 26, 2023
%% Simulation of the Simulink model
simOut = sim('sol_coll','StartTime','34200','StopTime','56788'); % Run of the Simulink model
% StartTime; Start time of the simulation
% StopTime; Stop time of the simulation
t = simOut.tout; % Extraction the return time vector of the simulation from
% the Simulink.SimulationOutput object, which name is simOut
y1 = simOut.yout{1}.Values.Data; % Collector outlet temperature calculated with Simulink model,
Tou(t), °C
y2 = simOut.yout{2}.Values.Data; % Measured collector outlet temperature, Tou(t) °C
%% Plot of the measured and the Simulink model calculated temperature
plot(t/3600,y1,t/3600,y2); % Plot of temperature vectors
xlabel('Time, hour'); % Horizontal axis label
ylabel('Temperature, °C'); % Vertical axis label
legend('Tou(t) calculated','Tou(t) measured'); % Legend

grid on; % Display axes grid lines
%% Extracted the Tou calculated
T = table(t, y1, 'VariableNames', {'time','Temperature'});
```



### Appendix 3. Parameter file and Data file required for the simulation (M-file) (2<sup>nd</sup> Day)

```
% Simulate the Simulink model of the flat-plate solar collector
% and plot the measured and calculated temperatures
% MATLAB code file name: run_sol_coll.m
% Parameters and hot water extraction function for modelling and simulation
% a flat-plate solar collector
% MATLAB code file name: collp2.m
%% By: Dr. János BUZÁS
% Hasna Saadi
% Department of Mechatronics, Institute of Technology
% Hungarian University of Agriculture and Life Sciences
% April 26, 2023
Ac = 1.92; % collector absorber surface, m^2
eta= 0.80; % optical efficiency of the collector,(dimensionless)
roc= 1050; % density of the collector heat transfer medium, kgm-3
        % (A 1:1 mixture of propylene glycol and distilled water)
cc = 3600; % specific heat of the collector heat transfer medium, Jkg-1K-1
Vc = 0.025; % volume of heat transfer medium in the collector, m^3
C =roc*cc*Vc; % heat capacity of the heat transfer medium in the collector, JK-1
Ul = 35; % total heat loss factor of the collector, Wm-2K-1
vc = 4.9166e-5; % volume flow of the collector circuit, m^3 s-1

Data Matrix U= [.....];

% The name of the MATLAB Code file containing the parameters of the Simulink model: collp2.m
% The file containing the measured data matrix for the simulation: s1990503.m
% The name of the Simulink model file: sol_coll.slx
%% By: Dr. János BUZÁS
% Hasna Saadi
% Department of Mechatronics, Institute of Technology
% Hungarian University of Agriculture and Life Sciences
% April 26, 2023
%% Simulation of the Simulink model
simOut = sim('sol_coll','StartTime','30596','StopTime','58626'); % Run of the Simulink model
        % StartTime; Start time of the simulation
        % StopTime; Stop time of the simulation
t = simOut.tout; % Extraction the return time vector of the simulation from
        % the Simulink.SimulationOutput object, which name is simOut
y1 = simOut.yout{1}.Values.Data; % Collector outlet temperature calculated with Simulink model,
Tou(t), °C
y2 = simOut.yout{2}.Values.Data; % Measured collector outlet temperature, Tou(t) °C
%% Plot of the measured and the Simulink model calculated temperature
plot(t/3600,y1,t/3600,y2); % Plot of temperature vectors
xlabel('Time, hour'); % Horizontal axis label
ylabel('Temperature, °C'); % Vertical axis label
legend('Tou(t) calculated','Tou(t) measured'); % Legend
title('Temperatures 2nd Day Experiments') % Add a title to the plot
grid on; % Display axes grid lines
%% Extracted the Tou calculated
idx = mod(t - t(1), 5) == 0;
y1_5sec = y1(idx);
t_5sec = (t(1) + (0:5:(numel(y1_5sec)-1)*5));
```

#### Appendix 4. Parameter file and Data file required for the simulation (M-file) (3<sup>rd</sup> Day)

```
% Parameters and hot water extraction function for modelling and simulation
% a flat-plate solar collector
% MATLAB code file name: collp2.m
%% By: Dr. János BUZÁS
% Hasna Saadi
% Department of Mechatronics, Institute of Technology
% Hungarian University of Agriculture and Life Sciences
% April 26, 2023
Ac = 1.92; % collector absorber surface, m^2
eta= 0.80; % optical efficiency of the collector,(dimensionless)
roc= 1050; % density of the collector heat transfer medium, kgm-3
      % (A 1:1 mixture of propylene glycol and distilled water)
cc = 3600; % specific heat of the collector heat transfer medium, Jkg-1K-1
Vc = 0.025; % volume of heat transfer medium in the collector, m^3
C =roc*cc*Vc; % heat capacity of the heat transfer medium in the collector, JK-1
Ul = 35; % total heat loss factor of the collector, Wm-2K-1
vc = 4.9166e-5; % volume flow of the collector circuit, m^3 s-1

Data Matrix U= [.....];

% Simulate the Simulink model of the flat-plate solar collector
% and plot the measured and calculated temperatures
% MATLAB code file name: run_sol_coll.m
% The name of the MATLAB Code file containing the parameters of the Simulink model: collp2.m
% The file containing the measured data matrix for the simulation: s1990503.m
% The name of the Simulink model file: sol_coll.slx
%% By: Dr. János BUZÁS
% Hasna Saadi
% Department of Mechatronics, Institute of Technology
% Hungarian University of Agriculture and Life Sciences
% April 26, 2023
%% Simulation of the Simulink model
simOut = sim('sol_coll','StartTime','30597','StopTime','50637'); % Run of the Simulink model
      % StartTime; Start time of the simulation
      % StopTime; Stop time of the simulation
t = simOut.tout; % Extraction the return time vector of the simulation from
      % the Simulink.SimulationOutput object, which name is simOut
y1 = simOut.yout{1}.Values.Data; % Collector outlet temperature calculated with Simulink model,
Tou(t), °C
y2 = simOut.yout{2}.Values.Data; % Measured collector outlet temperature, Tou(t) °C

%% Plot of the measured and the Simulink model calculated temperature
plot(t/3600,y1,t/3600,y2); % Plot of temperature vectors
xlabel('Time, hour'); % Horizontal axis label
ylabel('Temperature, °C'); % Vertical axis label
legend('Tou(t) calculated','Tou(t) measured'); % Legend
title('Temperatures 3 rd Day Experiments') % Add a title to the plot
grid on; % Display axes grid lines
%% Extracted the Tou calculated
idx = mod(t - t(1), 5) == 0;
y1_5sec = y1(idx);
t_5sec = (t(1) + (0:5:(numel(y1_5sec)-1)*5));
```